

Document downloaded from:

<http://hdl.handle.net/10251/145865>

This paper must be cited as:

Rosa-Tellez, S.; Anoman, A.; Flores-Tornero, M.; Toujani, W.; Alseek, S.; Fernie, A.; Nebauer, SG.... (02-2). Phosphoglycerate Kinases Are Co-Regulated to Adjust Metabolism and to Optimize Growth. *PLANT PHYSIOLOGY*. 176(2):1182-1198.
<https://doi.org/10.1104/pp.17.01227>



The final publication is available at

<https://doi.org/10.1104/pp.17.01227>

Copyright American Society of Plant Biologists

Additional Information

1 **Short Title.** PGKs are co-regulated to adjust central metabolism

2

3

4 **Author to whom all correspondence should be sent:** Roc Ros Palau

5

6 **Address:** Departament de Biologia Vegetal, Facultat de Farmàcia, Universitat de
7 València. Av. Vicent Andrés Estellés S/N, 46100 Burjassot (Valencia), Spain

8

9 **Telephone number:** 34-963543197

10

11 **e-mail address:** roc.ros@uv.es

12

13 **Research Area most appropriate for the paper:** Biochemistry and Metabolism.

14

15

16 **Focus Issue.** Metabolism

17
18
19
20
21
22
23
24
25
26
27
28
29
30
31
32
33
34
35
36
37
38
39
40
41
42
43
44
45
46
47
48
49
50
51
52

Phosphoglycerate kinases are co-regulated to adjust metabolism and to optimize growth

Sara Rosa-Télez^{a,b}, Armand Djoro Anoman^{a,b}, María Flores-Tornero^{a,b}, Walid Toujani^{a,b}, Saleh Alseek^c, Alisdair R. Fernie^c, Sergio G. Nebauer^d, Jesús Muñoz-Bertomeu^{a,b}, Juan Segura^{a,b}, Roc Ros^{a,b}

^aDepartament de Biologia Vegetal. Facultat de Farmàcia. Universitat de València. Spain.

^bEstructura de Recerca Interdisciplinària en Biotecnologia i Biomedicina (ERI BIOTECMED).

Universitat de València. Dr Moliner 50, 46100 Burjassot, Spain.

^cMax Planck Institut für Molekulare Pflanzenphysiologie, 14476 Potsdam-Golm, Germany.

^dDepartamento de Producción vegetal. Universitat Politècnica de València. Valencia. Spain

List of authors contributions.

S.R.T. performed most of the experiments and analyzed the data. A. D. A., M. F-T., W.T., S.A. and S.G.N. performed some of the experiments and analyzed the data. A. R. F., J.S. and J. M-B supervised the experiments and provided technical assistance. R.R. conceived the project and wrote the article with contributions of J.S. A.R.F, S.G.N and S.R.T.

Funding information: This work has been funded by the Spanish Government and the European Union: FEDER/ BFU2012-31519 and FEDER/ BFU2015-64204R, FPI fellowship to S. R-T and the Valencian Regional Government: PROMETEO II/2014/052.

ONE SENTENCE SUMMARY. Photosynthetic and glycolytic phosphoglycerate kinase mutants are transcriptionally co-regulated to achieve metabolic homeostasis and to optimize growth in Arabidopsis.

Corresponding Author e-mail: Roc Ros Palau (roc.ros@uv.es)

53

54

55 **ABSTRACT**

56 In plants, phosphoglycerate kinase (PGK) converts 1,3-bisphosphoglycerate into 3-
57 phosphoglycerate (3-PGA) in glycolysis, but also participates in the reverse reaction in
58 gluconeogenesis and the Calvin-Benson cycle. In the databases we found three genes
59 that encode putative PGKs. PGK1 was localized exclusively in the chloroplasts of
60 photosynthetic tissues, while PGK2 was expressed in the chloroplast/plastid of
61 photosynthetic and non-photosynthetic cells. PGK3 was ubiquitously expressed in the
62 cytosol of all studied cell types. Measurements of carbohydrate content and
63 photosynthetic activities in PGK mutants and silenced lines corroborated that PGK1
64 was the photosynthetic isoform, while PGK2 and PGK3 were the plastidial and
65 cytosolic glycolytic isoforms, respectively. The *pgk1.1* knock-down mutant displayed
66 reduced growth, lower photosynthetic capacity and starch content. The *pgk3.2* knock-
67 out mutant was characterized by a reduced growth, but a higher starch levels than the
68 wild-type. The *pgk1.1 pgk3.2* double mutant was bigger than *pgk3.2*, and displayed an
69 intermediate phenotype between the two single mutants in all measured biochemical
70 and physiological parameters. Expression studies in *PGK* mutants showed that *PGK1*
71 and *PGK3* were down-regulated in *pgk3.2* and *pgk1.1*, respectively. These results
72 indicate that the down-regulation of photosynthetic activity could be a plant strategy
73 when glycolysis is impaired to achieve metabolic adjustment and optimize growth. The
74 double mutants of *PGK3* and the triose-phosphate transporter (*pgk3.2 tpt3*) displayed a
75 drastic growth phenotype, but were viable. This implies that other enzymes or non-
76 specific chloroplast transporters could provide 3-PGA to the cytosol. Our results
77 highlight both the complexity and the plasticity of the plant primary metabolic network.

78

79

80

81

83 **INTRODUCTION**

84 Glycolysis was the first metabolic pathway to be fully elucidated biochemically in the
85 1940s (Plaxton, 1996). It is a central pathway in most living organisms, where it
86 provides energy in the form of ATP and reducing power, pyruvate to fuel the
87 tricarboxylic acid cycle (TCA), and precursors for secondary metabolism, amino acid,
88 and fatty acid biosynthesis (Plaxton, 1996). In plants glycolysis is more complex than in
89 animals, since it occurs independently in two compartments, the plastid and the cytosol.
90 Besides, according to the genome databases (<https://www.arabidopsis.org/>), there is
91 more than one isoform for each glycolytic reaction, and some of them are represented
92 by more than 40 annotations. In spite of the important advances made in the functional
93 characterization of both cytosolic and plastidial glycolytic enzymes (Sparla et al., 2005;
94 Fermani et al., 2007; Muñoz-Bertomeu et al., 2009; Chen and Thelen, 2010; Prabhakar
95 et al., 2010; Zhao and Assmann, 2011; Guo et al., 2012; Wakao et al., 2014), the
96 relative contribution and the degree of integration of both pathways in different cell
97 types are still far from being completely understood. In addition, some of the reactions
98 of the plastidial glycolytic pathway are shared by the Calvin-Benson cycle although
99 operating in the opposite direction. Specifically, glyceraldehyde-3-phosphate
100 dehydrogenase (GAPDH) and phosphoglycerate kinase (PGK) could participate in the
101 same compartment and/or at the same time in photosynthetic and
102 glycolytic/gluconeogenic reactions (Fig. 1). For this reason, the functional
103 characterization of both GAPDH and PGK isoforms is of crucial importance.

104 Plant GAPDH isoforms have been extensively characterized at genetic, biochemical and
105 molecular levels (Sparla et al., 2005; Hajirezaei et al., 2006; Fermani et al., 2007;
106 Holtgreffe et al., 2008; Muñoz-Bertomeu et al., 2009, 2010; Guo et al., 2012; Guo et al.,
107 2014; Anoman et al., 2015; Han et al., 2015). However, little attention has been paid to
108 the functional characterization of PGKs. These enzymes are essential in the metabolism
109 of most living organisms and their sequence has remained highly conserved throughout
110 evolution (Longstaff et al., 1989). They catalyze the reversible transfer of a highly
111 energetic phosphate group at position one of the 1,3-bisphosphoglycerate to ADP to
112 give rise to 3-phosphoglycerate (3-PGA) and ATP, and *vice versa*. PGKs from different
113 species have been isolated in both animals and plants (Krietsch and Bucher, 1970;
114 McCarrey and Thomas, 1987; Longstaff et al., 1989; Kopke-Secundo et al., 1990;
115 McMorro and Bradbeer, 1990; Lobler, 1998). Two PGK isoforms (PGK1 and PGK2)
116 encoded by two genes have been identified in humans. PGK1 is expressed in all somatic
117 cells, including red blood cells (Willard et al., 1985; McCarrey and Thomas, 1987;
118 Chiarelli et al., 2012), while PGK2 is sperm-cell specific (Boer et al., 1987). PGK1 has
119 been implicated in the metabolism of tumor cells (Lay et al., 2000; Hwang et al., 2006;
120 Zieker et al., 2008, 2010; Ai et al., 2011), and also in nuclear DNA replication and
121 repair (Popanda et al., 1998). PGK2 is essential for sperm motility and fertility
122 (Danshina et al., 2010).

123 In plants, PGKs are involved in not only glycolysis/gluconeogenesis but also in
124 photosynthetic carbon metabolism. Two highly conserved PGK isoforms were initially
125 identified in wheat (Longstaff et al., 1989). One of them being located primarily in the
126 cytosol, while the other was plastid-localized (Anderson and Advani, 1970). Although
127 the two PGKs could theoretically catalyze both the forward and reverse reactions, it was
128 assumed that the cytosolic isoform is involved in glycolysis and gluconeogenesis, while
129 the plastidial isoform participates, at least in photosynthetic cells, in both the Calvin-

130 Benson cycle and plastidial glycolysis (Anderson et al., 2004). However, this latter
131 assumption has not been thoroughly investigated to date. Subsequently, a second
132 cytosolic PGK isoform from *Helianthus annuus* was cloned (Troncoso-Ponce et al.,
133 2012), and in the Arabidopsis genome an additional putative PGK isoform with a N-
134 terminal plastid/chloroplast localization signal was identified (Ouibrahim et al., 2014).
135 The presence of two PGKs in the plastid/chloroplast could lead to a specialization so
136 that one of them could be involved in photosynthesis and the other in glycolysis, which
137 seems to be the case of GAPDH isoforms (Anoman et al. 2015). Indeed a mutant of one
138 of the Arabidopsis plastidial isoforms (At1g56190; *AtPGK2*) has been described as
139 lethal (Myouga et al., 2010; Ouibrahim et al., 2014), which suggests that the two
140 plastidial isoforms are not functionally redundant and likely play different roles in plant
141 metabolism. Moreover, chloroplastic and cytosolic PGKs proteins were localized in the
142 nucleus by immunocytolocalization experiments in peas (Anderson et al., 2004) which
143 is in keeping with the presence of functional nuclear localization signals in the cytosolic
144 PGK (Brice et al., 2004). This fact has led to the hypothesis that PGKs are able to act as
145 “moonlighting” proteins playing other roles apart from their participation in
146 metabolism. Accordingly, plastidial PGK2 has been shown to play a role in tolerance to
147 abiotic (Liu et al., 2015; Joshi et al., 2016) and biotic (Ouibrahim et al., 2014) stresses.
148 PGK2 has proven to be necessary for watermelon mosaic virus infection (Ouibrahim et
149 al., 2014). Specifically, PGK2 could mediate the transport of viruses to the chloroplast
150 (Lin et al., 2007; Cheng et al., 2013). The *in vitro* regulation of some PGK isoforms has
151 been studied (Troncoso-Ponce et al., 2012; Morisse et al., 2014). It has been shown that
152 the chloroplastic isoform of *Chlamydomonas reinhardtii* could be light-regulated by
153 thioredoxins (Morisse et al., 2014). Furthermore, at the biochemical level, glycolytic
154 PGKs activity has been reported to increase in sunflower developing embryos in
155 conjunction with the oil content (Troncoso-Ponce et al., 2009). It has also been shown
156 that PGK and enolase are two of the activities implicated in the differences in oil
157 content between standard and low oil content sunflower lines (Troncoso-Ponce et al.,
158 2010). Yet to date, no genetic or molecular evidence has been found to support the
159 metabolic function of specific PGKs. In this work, we have followed a loss-of-function
160 approach to functionally characterize all the glycolytic and photosynthetic isoforms
161 annotated in the Arabidopsis genome at both molecular and physiological levels. We
162 unraveled the specific contribution of each isoform to the primary metabolism of aerial
163 parts (AP) and roots, and concluded that both glycolytic and photosynthetic isoforms
164 are co-regulated to maintain the equilibrium between catabolic and anabolic processes.

165

166 RESULTS

167 Expression analysis and subcellular localization of the PGK family

168 In the Arabidopsis Information Resource database (TAIR; <http://www.arabidopsis.org>)
169 we found three genes encoding putative PGKs: At3g12780, At1g56190 and At1g79550.
170 According to the literature we named the proteins coded by these genes PGK1, PGK2
171 and PGK3, respectively. PGK1 displays 91% and 84% of amino acid identity with
172 PGK2 and PGK3, respectively, while the amino acid identity between PGK2 and PGK3
173 is 85%. The three isoforms show 100% identity in all residues that form the putative
174 catalytic site and the ligand binding domain (Supplemental Fig. S1A). The cladogram
175 confirmed that PGK1 and PGK2 are more closely related to one another than to PGK3
176 (Supplemental Fig. S1B). We next assessed the expression patterns of the *PGK* family
177 genes by quantitative real-time (RT) PCR and by analysis of promoter-GUS fusions in

178 both seedlings and adult plants. *PGK1* was expressed mainly in the leaves, and very
179 poorly in roots at both seedling and adult stages (Fig. 2A and B). *PGK2* was also
180 expressed mainly in leaves especially at the seedling stage, but at the adult stage its
181 relative expression in roots, siliques and flowers was higher than that of *PGK1*. By
182 contrast to *PGK1* and *PGK2*, *PGK3* was highly expressed in roots, especially at the
183 seedling stage. At the adult stage its expression pattern was the most homogeneous of
184 all three PGKs, being expressed similarly in all organs studied. These data confirm
185 publically available microarray expression data ([http://bar.utoronto.ca/efp/cgi-](http://bar.utoronto.ca/efp/cgi-bin/efpWeb.cgi)
186 [bin/efpWeb.cgi](http://bar.utoronto.ca/efp/cgi-bin/efpWeb.cgi)). The promoter-GUS analysis revealed a generalized expression of
187 *PGK1* in leaves and cotyledons, especially in guard cells and the surroundings of the
188 vasculature, in petals and sepals, and confirmed the lack of *PGK1* expression in
189 reproductive organs and roots (Fig. 2C and Supplemental Fig. S2). *PGK2* was strongly
190 expressed in leaf veins and margins, in the root vasculature, and in floral organs
191 (pedicel, petals, sepals and stigma) (Fig. 2C and Supplemental Fig. S3). *PGK3* was
192 homogeneously expressed in all plant tissues with a high expression in veins and distal
193 zones of leaves, and all over the roots, siliques and flowers (Fig. 2C and Supplemental
194 Fig. S4). According to the ChloroP prediction server
195 (<http://www.cbs.dtu.dk/services/ChloroP/>), both PGK1 and PGK2 harbor a N-terminal
196 plastid/chloroplast localization signal (Emanuelsson et al., 1999). To investigate the
197 subcellular localization of the PGK family proteins, we stably expressed PGK-GFP
198 fusion protein constructs under the control of the PGKs endogenous promoters in
199 *Arabidopsis* (*ProPGK1:PGK1-GFP*, *ProPGK2:PGK2-GFP*, *ProPGK3:PGK3-GFP*).
200 PGK1 was expressed mainly in the chloroplasts of mesophyll cells and no signal was
201 observed in roots (Fig. 3). PGK2 was expressed in leaf plastids/chloroplasts. In roots,
202 PGK2 was not homogeneously expressed, but displayed a high expression in the
203 columella plastids. PGK3 was similarly expressed in the cytosol of both root and leaf
204 cells (Fig. 3). PGK3 could also be localized in the nucleus as confirmed by the nuclear
205 Hoechst marker (Supplemental Fig. S5).

206 **Phenotypic characterization of PGK mutants**

207 In order to shed light on the *in vivo* function of *PGKs*, a loss-of-function approach was
208 followed. T-DNA insertion lines for each *PGK* gene were identified in the databases.
209 The genomic location of the T-DNA insertions was verified by PCR with genomic
210 DNA and sequencing of PCR products (Fig. 4A and Supplemental Table S1). In *pgk1.1*
211 (GK_172A12) and *pgk1.2* (GK_908E11), the T-DNA insertions were located in the
212 5'UTR region (Fig. 4A). In *pgk2.1* (SALK_016097), the T-DNA insertion was located
213 in the first exon. In *pgk3.1* (SALK_062377) and *pgk3.2* (SALK_066422), the T-DNA
214 insertion was located in the fourth and fifth exon, respectively (Fig. 4A). Based on PCR
215 genotyping, the segregation analysis of about 200 seeds from self-fertilized
216 heterozygous plants for *PGK1* or *PGK3* mutant alleles *pgk1.1*, *pgk1.2*, *pgk3.1* and
217 *pgk3.2* displayed a typical Mendelian ratio of 1:2:1 [homozygous mutant: heterozygous:
218 wild-type (WT)]. RT-PCR analysis indicated that *PGK3* mutants were knock-out while
219 both *PGK1* mutants were knock-down (Fig. 4B). The mutant *pgk1.1* showed the lowest
220 *PGK1* expression and was chosen for further analysis (Fig. 4B).

221 The analysis of *pgk2.1* seedlings from self-fertilized heterozygous plants identified a
222 population of albino individuals when grown in plates with sucrose, which were
223 associated with the mutant homozygous genotype (mutant: WT phenotype ratio of 1:3).
224 This phenotype could indicate that the homozygous *pgk2.1* individuals are lethal, as
225 formerly observed in two different T-DNA insertion lines (SALK_016097 and
226 Salk_071724) (Myouga et al., 2010; Ouibrahim et al., 2014). *PGK2* expression in

227 *pgk2.1* was null (Fig. 4B). However, it was not possible to complement *pgk2.1* with
228 any of the different constructs used herein (a *PGK2* cDNA under the control of the 35S
229 or native *PGK2* promoter, a genomic *PGK2* sequence) suggesting that there was
230 probably more than one mutation associated with this line. Attempts to separate the
231 albino phenotype from the T-DNA insertion by back-crosses with WT individuals were
232 unsuccessful. As a genotype-phenotype correlation was not found, this mutant allele
233 was discarded for further experiments. Instead *PGK2* down-regulated lines were made
234 using artificial microRNAs (amiRNA). Fifteen lines overexpressing an amiRNA
235 directed against the *PGK2* in a WT background were obtained, and two lines were
236 selected on the basis of having the lowest *PGK2* transcript level (Supplemental Fig.
237 S6A).

238 Growth parameters were quantified in homozygous mutants at different stages of
239 development *in vitro* or in greenhouse conditions (Fig. 5). *PGK3* mutants presented a
240 significant reduction in all growth parameters measured as compared to WT controls at
241 all growth stages analyzed (Figs. 5A, B, C and D). *pgk1.1* displayed a trend to a reduced
242 growth in plates which was significant in greenhouse conditions, where irradiance was
243 higher (Fig. 5C). To support that the reduction of growth in *pgk1.1* was associated with
244 a lower *PGK1* expression, amiRNA silenced lines were obtained (Supplemental Fig.
245 S6B). The reduced growth of these lines corroborated the relation between *PGK1*
246 expression level and growth (Figs. 5A, B and C). The *amiRNA-PGK2* lines displayed
247 milder phenotypes than mutants from other genes, and only one of the two selected lines
248 with the lowest *PGK2* expression level showed a significant reduction of rosette fresh
249 weight as compared to controls (Fig. 5C). No changes in photosynthetic activities were
250 observed in these lines (Supplemental Table S2).

251 Lower photosynthetic capacity was observed in 20- and 30-day-old *pgk1.1* plants, as
252 inferred from the decreased net photosynthetic rate, and effective and maximum
253 photochemical yield of PSII (Table 1). These results, together with the observed
254 plastidial localization of PGK1, would suggest a role of this isoform in the Calvin-
255 Benson cycle. Accordingly, lower starch content was measured in *pgk1.1* plants (Figure
256 6A). No differences in photosynthetic parameters were observed in 20-day-old plants of
257 *pgk3.2* in comparison to WT (Table 1). In this mutant, starch levels were higher than in
258 WT. These results alongside the localization studies, would support the hypothesis that
259 PGK3 is involved in the cytosolic glycolysis. However, in 30-day-old plants, the
260 photosynthetic activity decreased in *pgk3.2*, which suggest that low cytosolic glycolytic
261 activity affects photosynthesis in the long term (Table 1).

262 To further corroborate the genotype-phenotype correlation of *pgk1.1* and *pgk3.2*, we
263 transformed the mutants with a construct carrying the native *PGK1* or *PGK3* cDNA
264 under the control of the endogenous or the 35S promoter, respectively. We were able to
265 complement the growth phenotypes associated with both the *pgk1.1* and *pgk3.2*
266 mutations (Fig. 5E). Accordingly, the photosynthetic parameters were completely or
267 partially recovered in *pgk1.1* and *pgk3.2* complemented lines (Table 1).

268

269 **Metabolomics profile of down-regulated *PGK* lines**

270 To understand the contribution of the PGKs to the primary metabolism, we studied the
271 metabolomics profile of the *PGK* mutants. A clearly altered metabolite content in the
272 AP and roots of mutants was observed (Fig. 7 and Supplemental Table S3).

273 In the *pgk1.1* AP, the most important changes were found in the amino acid pool. Many
274 amino acids (threonic acid, alanine, aspartate, proline) increased by more than 40% as
275 compared to the WT (Fig. 7 and Supplemental Table S3). Sugars were not so strongly
276 affected and none of them varied by more than 40% as compared to the WT, although
277 glucose and sucrose increased by 29% and 24%, respectively. In roots, the pattern of
278 metabolite modifications differed from that obtained in the AP and the sugar levels were
279 especially affected (Fig. 7 and Supplemental Table S4), with all the quantified sugars
280 and sugar derivatives, with the exception of glyceraldehyde-3-phosphate, being
281 significantly increased. Quantitatively, the most striking changes were those in the
282 levels of fructose (103% increase) and glucose (71% increase).

283 The *pgk3.2* AP showed a general increase in amino acids and sugar levels (Fig. 7 and
284 Supplemental Table S3). Of the 21 amino acids detected, the increases were significant
285 in seven, while the decreases were significant only in three. Some, e.g., glutamine and
286 *O*-acetyl serine, increased by more than 40%. In addition, increases were observed in
287 more than half of the quantified sugars, and the increases in fructose (up to 164%) and
288 glucose (113%) levels were particularly noteworthy. In the *pgk3.2* roots the most
289 prominent changes were observed in certain organic acids, e.g, succinic and citric,
290 which increased 52% and 108%, respectively (Fig. 7 and Supplemental Table S4). As
291 for soluble sugars, the increase was higher than that observed in the AP, especially the
292 increases in glucose (167%) and fructose (287%). Similar changes in the *pgk3.2* AP and
293 roots were also found in the glyceric and phosphoric acid contents, which decreased in
294 both organs.

295 Significant changes were found in the *amiRNA-PGK2* lines, but they were generally less
296 dramatic than in the other studied mutants (Fig. 7 and Supplemental Tables S3 and S4).
297 In the *amiRNA-PGK2* AP, there was a general trend towards a decrease in the
298 metabolite content, but only raffinose reduced by more than 40%. In roots, an
299 increasing trend was noted in metabolite content but, once again, changes were not as
300 drastic as in the other mutant lines (approximately 10% different from WT levels).

301

302 **The *PGK1* and *PGK3* double mutation compensates the growth defects and** 303 **metabolic disorders of single mutants**

304 Transcriptomics data provided in the databases ([http://bar.utoronto.ca/efp/cgi-](http://bar.utoronto.ca/efp/cgi-bin/efpWeb.cgi)
305 [bin/efpWeb.cgi](http://bar.utoronto.ca/efp/cgi-bin/efpWeb.cgi)) and our own RNA-seq data indicate that *PGK1* is the most abundant
306 PGK transcript in Arabidopsis leaves (*PGK1*:945, *PGK2*:118, *PGK3*:102 counts in the
307 AP). PGK cytosolic activity accounts for 5-10% of total PGK activity in barley and
308 spinach, while chloroplastic activities account for 90-95% (Kopke-Secundo et al., 1990;
309 McMorro and Bradbeer, 1990). These activity data well agree with the transcript
310 abundance of PGK isoforms in the Arabidopsis AP.

311 We observed a significant reduction in PGK total activity in the AP of 20-day-old
312 *pgk1.1* seedlings and a non-significant trend to a reduction in *pgk3.2* (Figure 6B). Since
313 *PGK1* is the most abundant transcript in the AP, changes in the activity of other
314 isoforms could be masked or be difficult to detect in this organ. However in roots,
315 where *PGK3* transcripts are the most abundant (*PGK1*:46, *PGK2*:62, *PGK3*:262 counts
316 in the roots), a reduction of about 75% of total PGK activity was observed in *pgk3.2*,
317 while no activity changes were observed in *pgk1.1* as compared to WT. Since *pgk3.2* is
318 knock-out, the remaining 25% of PGK activity measured in the mutant roots could be to
319 both *PGK1* and *PGK2* isoforms. There were no differences in *amiPGK2* PGK activity

320 in either AP or roots, which may imply that the silencing is not absolute and/or that it is
321 a global minority isoform in both organs, as evidenced by the transcriptomics data.

322 In 30-day-old plants, a significant reduction in the AP PGK activity was observed in
323 both *pgk1.1* and *pgk3.2*. Besides, this reduction was more marked in 30-day-old than in
324 20-day-old *pgk1.1* plants as compared to controls. Differences in total PGK activity in
325 the mutant at seedling (20 day-old) and adult (30-day-old) stage could be related to
326 changes in PGK gene expression. For this reason, we studied the *PGK* family gene
327 expression in the different mutant backgrounds at different developmental stages (Fig.
328 6C). At the seedling stage only *PGK1* expression was slightly reduced in *pgk3.2*.
329 However, in adult plants *PGK1* and *PGK3* expressions were dramatically down-
330 regulated in *pgk3.2* and *pgk1.1*, respectively. The reduction in photosynthetic activity
331 observed in 30-day-old *pgk3.2* (Table 1) could be associated with the repression of
332 *PGK1* in the mutant at this developmental stage.

333 All these results could indicate that PGKs expression is regulated at the transcriptional
334 level to adjust metabolism. To corroborate this hypothesis, a double mutant of *pgk1.1*
335 and *pgk3.2* was generated and subsequently studied. *pgk1.1 pgk3.2* did not show more
336 dramatic phenotypes as compared to single mutants. On the contrary, the *pgk1.1 pgk3.2*
337 growth phenotype was less severe than that of *pgk3.2* (Figs. 5C and D), and the starch
338 levels and photosynthetic activities were less affected as compared to *pgk1.1* (Fig. 6A
339 and Table 1). Double mutants improved their growth and photosynthetic activities as
340 compared to single mutants as plants were getting older, suggesting a long term
341 compensatory effect of the double mutation (Figs. 5A, B, C and D, Table 1).

342 The metabolite analysis confirmed a compensatory effect of the double mutation (Fig. 7
343 and Supplemental Tables S3 and S4). For instance, some metabolites such as alanine
344 and proline, increased in the *pgk1.1* AP by more than 40% compared to WT, but did not
345 differ significantly in the *pgk3.2* AP. In *pgk1.1 pgk3.2*, the AP contents of such
346 metabolites did not significantly differ from those in the WT either (Fig. 7 and
347 Supplemental Table S3). In the *pgk3.2* AP, the metabolites that varied more than 40%
348 but whose content did not differ with respect to WT in *pgk1.1*, were glutamine (80%)
349 and fructose (164%) (Fig. 7 and Supplemental Table S3). In *pgk1.1 pgk3.2*, the
350 glutamine content was significantly higher than in the control, but decreased to 30%,
351 whereas the fructose content did not show significant differences. Finally, the contents
352 of those metabolites that changed in the same direction in both single mutants (succinic
353 acid, aspartate, *O*-acetyl-serine, citric acid and glucose) were not superior in the double
354 mutant to those of the single mutants, but were rather intermediate or more similar to
355 WT. The trend described above for the AP was additionally observed in roots (Fig. 7
356 and Supplemental Table S4).

357

358 **Blocking the flux of 3-PGA between the plastid and the cytosol accentuates the** 359 ***pgk3.1* phenotypes**

360 PGK3 should provide the 3-PGA needed for the essential reactions of the glycolytic
361 cytosolic pathway. In spite of PGK3 being the sole cytosolic PGK isoform, the knock-
362 out *pgk3.2* was viable. The relative 3-PGA level was not reduced but increased in
363 *pgk3.2* plants compared to WT (Fig. 8A). We postulate that some of the 3-PGA needed
364 for respiration could be provided by plastidial glycolysis and be transported to the
365 cytosol by the triose phosphate transporter (TPT), the main carbon transporter in the
366 AP. To investigate this hypothesis, we interrupted the metabolite communication

367 between the cytosol and the plastids by generating a double knock-out mutant of *pgk3.2*
368 and TPT (*tpt3*), (Fig. 4A).

369 The *pgk3.2 tpt3* showed a more dramatic growth phenotype than the single mutants,
370 indicating an additive effect of the mutations (Fig. 8B). Accordingly, the starch level in
371 the AP of *pgk3.2 tpt3* was even higher than in *tpt3* (Fig. 8C). The metabolomics
372 analysis of the *pgk3.2 tpt3* AP indicated that there was a general increase in amino acid
373 content as observed in *pgk3.2* (Fig. 8D and Supplemental Table S5). It is worth
374 mentioning that serine and its derivatives (methionine and *O*-acetyl-serine) also
375 increased, which could indicate an activation of the plastidial phosphorylated pathway
376 of serine biosynthesis. When amino acids increased in both single mutants, an additive
377 effect was always observed in the double mutants. Interestingly, the glyceric and
378 phosphoric acid contents, which decreased dramatically in *pgk3.2*, increased in *tpt3*. In
379 *pgk3.2 tpt3*, these metabolites displayed an intermediate phenotype. Sugar levels
380 (glucose, mannose and fructose) increased in *pgk3.2* but were decrease in *tpt3*,
381 displaying intermediate values in *pgk3.2 tpt3*. Once again when sugar trends were
382 similar in both single mutants, the change became more marked in *pgk3.2 tpt3*. For
383 example, galactinol, *myo*-inositol, xylose and trehalose, which increased in both single
384 mutants were further increased in *pgk3.2 tpt3*. Thus the metabolomics analysis fully
385 corroborated the additive effect of the double mutation.

386

387 **DISCUSSION**

388 **Functions of the PGK isoforms and impact in plant development**

389 The study of the expression patterns of PGK family genes, as well as their intracellular
390 localization provided important information concerning their function in Arabidopsis.
391 Both PGK1 and PGK2 are plastid-localized, while PGK3 is localized in both the cytosol
392 and the nucleus. The nuclear localization of PGK3 corroborates previous findings in
393 peas (Anderson et al., 2004), which could indicate that this enzyme not only participates
394 in metabolism, but also performs additional functions, as previously demonstrated in
395 mammals. *PGK1* is almost exclusively expressed in photosynthetic tissues and *PGK3* is
396 quite uniformly expressed in all organs. The expression studies, along with the results
397 obtained in the metabolomics and photosynthetic analyses of the different lines (i.e.
398 lower levels of starch and photosynthetic activities in *pgk1.1*), clearly indicate that
399 PGK1 is a photosynthetic isoform, whereas PGK3 is the cytosolic glycolytic isoform.

400 The low values of the maximum quantum efficiency of PSII (Fv/Fm) in *pgk1.1* suggests
401 the existence of a photoinhibition or photosynthetic damage phenomenon. This negative
402 effect could be related to a reduced PGK1 activity in this mutant. PGK consumes most
403 of the ATP required in the Calvin-Benson cycle, so its low activity would limit the
404 regeneration of electron acceptors required for the operation of the photosynthetic
405 electron transport chain. The smaller *pgk1.1* size may be related to their lower
406 photosynthetic capacity and/or damage caused by photoinhibition. The negative effect
407 on mutant growth was observed more clearly under greenhouse conditions, where the
408 light intensity is higher than in growth chambers. In the greenhouse, the greater
409 photosynthetic capacity of the WT and/or its lesser photoinhibition could accentuate the
410 growth differences between the two lines.

411 *pgk3.2* showed the more dramatic reduction in growth of all the single mutants
412 characterized here. This may be related to the mutant incapacity to metabolize

413 carbohydrates for growth, since the starch and sugar levels in this mutant were higher
414 than in the WT. Thirty-day-old *pgk3.2* displayed symptoms of photoinhibition and a
415 dramatic reduction of *PGK1* expression along with a reduction in the photosynthetic
416 activity. The high levels of carbohydrates could have a negative feed-back effect on the
417 expression of photosynthetic genes (Paul and Pellny, 2003; Smith and Stitt, 2007; Stitt
418 et al., 2010; McCormick and Kruger, 2015) and thus a general inhibition of
419 photosynthesis.

420 PGK2 was plastid-localized, and is most probably a glycolytic isoform. Yet the high
421 *PGK2* expression in leaves raises the question of additional functions in photosynthetic
422 tissues, especially when compared with the low expression of the plastidial glycolytic
423 isoforms of GAPDH in this organ (Muñoz-Bertomeu et al., 2009). Phylogenetic studies
424 of plant PGKs indicate that photosynthetic and glycolytic isoenzymes have a common
425 origin and come from an ancestral eubacteria gene that duplicated and replaced the pre-
426 existing eukaryotic gene (Brinkmann and Martin, 1996; Archibald and Keeling, 2003).
427 This situation contrasts with that of the GAPDHs, where the glycolytic isoforms have
428 an eukaryotic origin (Petersen et al., 2003) whilst the photosynthetic enzymes are
429 prokaryotic in nature (Shih et al., 1986). The bacterial origin of both glycolytic and
430 photosynthetic PGKs could be relevant to both the enzyme activity and regulation, and
431 could be related with a greater versatility of these enzyme isoforms. While the
432 *Arabidopsis* genome has five plastidial and two cytoplasmic GAPDH isoforms, the
433 PGK only have one cytosolic and two plastidial isoforms, which indicates a greater
434 degree of specialization in the GAPDH than in the PGK family. A partially redundant
435 function of PGK2 in photosynthesis could explain the high level of gene expression in
436 leaves. However, the *amiRNA-PGK2* lines did not have any effect either on the
437 photosynthetic activity or on the starch content, which renders this hypothesis difficult
438 to prove.

439 In spite of the possible lethal phenotype of *pgk2.1* (this study, Myouga et al., 2010;
440 Ouibrahim et al., 2014), the *amiRNA-PGK2* lines displayed weaker metabolite changes
441 than the other mutants (Fig. 6). This suggests that either *pgk2.1* is not lethal or that
442 silenced lines have residual levels of PGK2 activity which are sufficient to maintain
443 them. There are other examples of enzymes whose insertional mutants are lethal and
444 whose silenced lines are viable (Cascales-Miñana et al., 2013). This fact reinforces the
445 idea that low transcription levels in *amiRNA* lines may mask the more dramatic
446 phenotypes observed in knock-out mutants, and, thus, other levels of enzyme
447 posttranscriptional and/or post-translational regulation (regulation by substrates and
448 other interacting proteins, enzyme biosynthesis turnover) may compensate for the low
449 transcription level. Hence, a silencing strategy may be of limited use for metabolic
450 enzymes. In any case, due to the lack of phenotypic complementation of *pgk2.1*, we
451 cannot rule out that other closely linked mutations may be partly responsible for the
452 observed lethal phenotype of this mutant.

453

454 **PGK1 and PGK3 are transcriptionally co-regulated to adjust metabolism**

455 We found a correlation between PGK gene expression and enzyme activities, which
456 indicates that transcription is an important mechanism of PGK regulation. The
457 importance of transcriptional regulation for PGKs may be related to their bacterial
458 origin and could be different from other metabolic enzymes of eukaryotic origin.

459 Since *pgk1.1* and *pgk3.2* single mutants displayed reduced growth, we expected this
460 reduction to be even more drastic in the double mutant as both photosynthetic and
461 glycolytic activities were affected. However, contrary to our expectations, *pgk1.1*
462 *pgk3.2* was bigger than *pgk3.2*, and displayed an intermediate phenotype between the
463 two single mutants in all measured biochemical and physiological parameters
464 (metabolite contents and photosynthetic activity). These results rule out an additive
465 effect of the double mutation and point rather towards a compensatory effect which
466 could be related to the co-regulated *PGK* expression in the single mutants. Thus, *PGK3*
467 expression is repressed in *pgk1.1* in late development stages. The reduced PGK activity
468 in this mutant compared to earlier stages might therefore be related to *PGK3* repression,
469 at least in part. The repression of genes involved in sugar catabolism has also been
470 observed in mutants with a low starch content, and has been associated with an adaptive
471 response to avoid reserve depletion (Blasing et al., 2005; Smith and Stitt, 2007).

472 Furthermore, the reduced PGK activity found in the AP of *pgk3.2* adult plants could be
473 due in part to *PGK1* repression. This repression would avoid the accumulation of
474 carbohydrates in *pgk3.2*, which could have an inhibitory effect on the photosynthetic
475 activity, and thus ultimately on growth. Our results indicate that when the glycolysis is
476 limited, the plant tends to readjust the rate of photosynthesis to compensate for the
477 effects caused by accumulation of carbohydrates, and *vice versa*. Therefore, reduced
478 photosynthetic activity in the double mutant in early stages would avoid the
479 accumulation of excess sugars as a result of a diminished glycolytic activity, which has
480 a beneficial effect on the long-term growth of the double mutant as compared to the
481 single mutants.

482 **PGK3 activity is by-passed in *pgk3* metabolism**

483 Since metabolism is a complex and dynamic process, it is difficult to predict the
484 metabolite changes associated with the lack of a certain enzyme activity, especially if
485 the same activity is displayed by different isoforms and in distinct compartments. PGK3
486 should be the main provider of cytosolic 3-PGA for the downstream reactions of
487 glycolysis, and thus for respiratory activity. Lack of PGK3 activity was associated to an
488 increase in soluble sugar (mainly glucose and fructose) and starch. These increases
489 could be caused by a reduced glycolytic activity which, in turn, slows down plant
490 growth. However, total 3-PGA content, the product of the PGK3 activity, increased in
491 *pgk3.2*. This could indicate that more 3-PGA is generated in *pgk3.2* by other reactions,
492 e.g., through a higher photosynthetic activity. However, this was not always the case,
493 since both photosynthetic activity and PGK1 expression were reduced in the adult
494 *pgk3.2* plants, in which 3-PGA was measured. Another possible route to increase 3-
495 PGA availability is via the plastidial glycolytic pathway which, as the increased *PGK2*
496 expression suggests, could have been more active in the *pgk3.2*. In the WT AP, the
497 triose-phosphates are transported from the plastid to the cytosol through the TPT (Fig.
498 1). We hypothesized that in *pgk3.2*, PGK2 activity is increased to produce more 3-PGA
499 in the plastid to by-pass the PGK3 reaction, which is then transported to the cytosol
500 through the TPT (Fig. 1). Once in the cytosol, 3-PGA could complete with glycolysis in
501 order to fuel the TCA cycle when necessary. The increased plastidial glycolytic activity
502 hypothesis could also be applicable to heterotrophic plastids. In root plastids, where
503 TPT activity is absent, 3-PGA can be potentially converted into phospho-*enol*-pyruvate
504 (PEP) by phosphoglycerate mutase and enolase (Prabhakar et al., 2010; Flores-Tornero
505 et al., 2017). PEP could be the metabolite transported from the plastid to complete
506 glycolysis in the cytosol. Indeed, it has been postulated that the PEP/Pi translocator acts
507 as a net importer of PEP into the chloroplast, but as a net exporter in root plastids

508 (Staehr et al., 2014) and probably in plastids from other non-photosynthetic tissues such
509 as embryos (Flores-Tornero et al., 2017).

510 The drastic phenotype of *pgk3.2 tpt3* would suggest that the TPT activity could, at least
511 in part, alleviate the PGK3 deficiency. In this double mutant, the 3-PGA formed by
512 photosynthesis or plastidial glycolysis in the AP could not be exported to the cytosol
513 and would mainly accumulate as starch as it does in the *tpt3* single mutant. Besides, the
514 measured increases in serine and derivatives (methionine and *O*-acetyl-serine), which
515 were already apparent in *tpt3*, could indicate an activation of the plastidial
516 phosphorylated pathway of serine biosynthesis to divert part of the 3-PGA flux towards
517 serine synthesis.

518 Since *pgk3.2 tpt3* is a double knock-out mutant that is still viable, there must be other
519 mechanisms able to supply the essential 3-PGA to the cytosol in the mutant AP. These
520 other possible mechanisms could include the inefficient 3-PGA transport through other
521 chloroplast membrane transporters of the phosphate translocator family, such as glucose
522 or xylulose-5-phosphate translocators (Fischer and Weber, 2002) or the involvement of
523 the non-phosphorylating cytosolic GAPDH, which produces 3-PGA from
524 glyceraldehyde-3-phosphate bypassing the PGK3 reaction (Rius et al., 2006). These
525 mechanisms whilst inefficient may be sufficient to maintain the mutants viability.

526 Evaluation of the metabolomics data from different lines can help to find those changes
527 in metabolite levels which can corroborate the above-postulated hypotheses and
528 establish the connections between different metabolic pathways. Several metabolites
529 changed in the opposite direction in the *pgk3.2* and *tpt3* single mutants, including
530 glucose, fructose and glycerate. As previous mentioned, the accumulation of glucose,
531 fructose and starch in *pgk3.2* may be caused by the impairment of their metabolism via
532 glycolysis. In *tpt3*, the low levels of soluble sugars most likely reflect the inhibition of
533 triose-phosphate transport to the cytosol, and as such a restricted substrate supply in
534 support of their formation. Carbohydrates thus instead accumulate in the form of starch,
535 a phenomenon that was also observed in *pgk3.2 tpt3*. Moreover, glyceric acid decreased
536 in *pgk3.2*, increased in *tpt3* and presented an intermediate value in the double mutant.
537 These reverse changes between *pgk3.2* and *tpt3* could be related to the strategy in
538 *pgk3.2* to redirect the glycolytic flux towards the plastid. Low glyceric acid levels in
539 the AP, could be the result of the conversion of this metabolite into 3-PGA by the
540 plastidial glycerate kinase to be transported to the cytosol through TPT (Fig. 1).
541 Interestingly, the phosphoric acid content also dramatically decreased in the *pgk3.2* AP,
542 but increased in *tpt3*. Given that it correlated with the inorganic phosphate levels, the
543 low phosphoric acid levels in the *pgk3.2* AP may be indicative of the high 3-PGA:Pi
544 exchange rate, which is, by contrast, disrupted in *tpt3*.

545

546 CONCLUSIONS

547 Our results provide new insights into the functions of PGK isoforms and how they are
548 regulated. The expression studies, along with the biochemical and physiological
549 characterization, demonstrate that PGK1 is the photosynthetic isoform, while PGK2 is
550 most probably involved in plastid glycolysis. PGK3 would be the cytosolic glycolytic
551 isoform.

552 The study of the double mutant supports both the complexity and the plasticity of the
553 primary metabolic network. Here it is emphasized that imbalances of photosynthetic

554 metabolism tend to be corrected by the regulation of the glycolytic routes and *vice*
555 *versa*. Therefore, results obtained in this work support that plastidial and cytosolic
556 metabolism are intimately connected, and that regulatory mechanisms exists which tend
557 to maintain the balance between catabolic and anabolic reactions in the central carbon
558 metabolism of plants.

559

560

561 **MATERIALS AND METHODS**

562 **Plant Material and Growth Conditions**

563 *Arabidopsis thaliana* seeds (ecotype Columbia-0) were supplied by the European
564 Arabidopsis Stock Center (Scholl et al., 2000). Seeds were sterilized and sown on 0.8%
565 agar plates containing one-fifth-strength Murashige and Skoog (1/5 MS) medium with
566 Gamborg vitamins buffered with 0.9 g/l MES (adjusted to pH 5.7 with Tris). After a 4-
567 day treatment at 4°C, plates were vertically placed in a growth chamber (IBERCEX,
568 V350, Spain) at 22°C under a 16 h day/8 h night photoperiod, 100 $\mu\text{mol m}^{-2} \text{s}^{-1}$. To
569 select the transgenic plants, half-strength MS plates supplemented with 0.5% sucrose
570 and appropriate selection markers were used. Some seeds were also grown under
571 greenhouse conditions in pots filled with a (1:1, v/v) mixture of vermiculite and
572 fertilized peat (KEKILA 50/50; kekkilä Iberia, S.L.) irrigated with demineralized water
573 as required. Trays were placed in a cold chamber (4°C) and were placed under the
574 greenhouse staging after 4 days. Growth conditions consisted of 16h light, 50-70%
575 relative humidity and an average temperature of 24°C during the daytime and 17°C
576 during the night. Whenever necessary, these conditions were supplied with artificial
577 light from sodium and mercury vapor lamps. For analyses, 18-30 day-old pre-bolting
578 material from plates or pots was harvested and separated into AP (including leaves and
579 cotyledons) and roots. Unless otherwise stated, the material was sampled at the middle
580 of the light period.

581

582 **Primers**

583 All primers used in this work are listed in Supplemental Table S6.

584 **Mutant Isolation and Characterization**

585 The mutant alleles of *PGK1* (At3g12780), *PGK2* (At1g56190), *PGK3* (At1g79550) and
586 *TPT* (At5g46110) were identified in the SIGnAL Collection database at the Salk
587 Institute (Alonso et al., 2003); GK_172A12 and GK_908E11 for *PGK1*, SALK_016097
588 for *PGK2*, SALK_062377 and SALK_066422 for *PGK3* and SALK_09334 for *TPT*.
589 Mutants were identified by PCR genotyping using gene-specific primers and left border
590 primers of the T-DNA insertion (Supplemental Table S6). The T-DNA insertions were
591 confirmed by sequencing the fragment amplified by the T-DNA internal primers and
592 gene specific primers (Supplemental Table S6).

593 **Cloning and Plant Transformation**

594 Standard methods were used to make the gene constructs (Sambrook and Russell,
595 2001). For gene promoter-GUS fusions, genomic DNA was PCR-amplified using
596 primers At3g12780PromHind3F and At3g12780PromSpeR for the *PGK1* promoter
597 (1508 bp), At1g56190PromNcoIR and At1g56190PromXbaIF for the *PGK2* promoter

598 (1466 bp), and At1g79550PromSpeIR and At1g79550PromHind3F for the *PGK3*
599 promoter (1284 bp). Plasmid pCAMBIA1303 was used to fuse the promoter fragments
600 to the β -Glucuronidase gene using the sites indicated in the respective primer names.

601 For promoter-PGK-GFP fusions, PGK cDNAs were PCR-amplified with the following
602 primers: At3g12780GFP-F and At3g12780GFP-R for *PGK1*; At1g56190GFP-F and
603 At1g56190GFP-R for *PGK2*; and At1g79550GFP-F and At1g79550GFP-R for *PGK3*.
604 PCR products were cloned in the pCR8/GW/TOPO plasmid (Invitrogen). These cDNAs
605 were subcloned in the plasmid pMDC83 under the control of the *35S* promoter (Curtis
606 and Grossniklaus, 2003) using the Gateway technology with clonase II (Invitrogen).
607 The pMDC83 plasmids allowed us to clone *PGK* cDNAs in frame with a green
608 fluorescent protein (GFP) cDNA at the C-term position (PGK1-GFP, PGK2-GFP,
609 PGK3-GFP). Promoter regions of PGKs previously cloned in pCAMBIA1303 were
610 PCR-amplified to introduce restriction sites (primers At3g12780PmeIProF and
611 At3g12780PromSpeR introduced *PmeI* and *SpeI* restriction sites into the *PGK1*
612 promoter; primers At1g56190FProPmeI and At1g56190RevProPacI introduced *PmeI*
613 and *PacI* restriction sites into the *PGK2* promoter; primers At1g79550ProPmeIFo and
614 At1g79550PromSpeIR introduced *PmeI* and *SpeI* restriction sites into the *PGK3*
615 promoter). Subsequently, the *35S* promoters of constructs in pMDC83 were exchanged
616 with the native promoters of *PGKs*, PCR-amplified from pCAMBIA1303 and digested
617 with the appropriate restriction enzymes. These vectors, called *ProPGK:PGKs*, were
618 used for PGKs expression and localization studies, and for the complementation of
619 *PGK1* and *PGK2* mutants. For *pgk3.2* complementation studies, the *Pro35S:PGK3-*
620 *GFP* construct in pMDC83 was used. Besides, *pgk2.1* was also transformed with a
621 construct carrying a 3718 bp genomic fragment which was PCR-amplified from BAC
622 *F14G9* using primers At1g56190ForGENO and At1g56190RevGENO. This fragment,
623 including 1466 nucleotides upstream of the ATG, was cloned in the pCR8/GW/TOPO
624 plasmid (Invitrogen), and was subsequently subcloned in the plasmid pMDC99 (Curtis
625 and Grossniklaus, 2003) using the Gateway technology with clonase II (Invitrogen).

626 Artificial microRNA (amiRNAs) were produced to target *PGK1* and *PGK2* using the
627 web microRNA designer (<http://wmd2.weigelworld.org/cgi-bin/mirnatools.pl>). The
628 amiRNAs were cloned according to the protocol by Rebecca Schwab in Prof. Weigel's
629 laboratory
630 (http://wmd2.weigelworld.org/themes/amiRNA/pics/Cloning_of_artificial_microRNAs.pdf)
631 using primers listed in Supplemental Table S6; then placed in the
632 pCR8/GW/TOPO plasmid (Invitrogen) and finally subcloned in the plasmid pMDC83
633 behind the *35S* promoter (Curtis and Grossniklaus, 2003). All PCR-derived constructs
634 were verified by DNA sequencing.

635 Various Arabidopsis WT and mutant lines were transformed with the different
636 constructs by the floral dipping method (Clough and Bent, 1998) with *Agrobacterium*
637 *tumefaciens* carrying *pSOUP*. For the amiRNA and GUS lines, WT were used.
638 Transformants were selected by antibiotic selection, while homozygous individuals in
639 complementation studies were identified by PCR genotyping using gene-specific
640 primers and left border primers of the T-DNA insertions listed in Supplemental Table
641 S6. At least four independent single insertion homozygous T3 lines were obtained for
642 all different constructs. After characterization by RT-PCR, two different lines were
643 selected for further analyses according to their expression level. We used both syngenic
644 WT lines, as well as WT Columbia 0, as controls for our studies. For amiRNAs, we
645 used the WT used for transformation with the amiRNAs as controls.

646

647 **RT-PCR and RNA-seq data**

648 RT-PCR was performed as previously described (Cascales-Miñana et al. 2013). Each
649 reaction was performed in triplicate with 1 μ L of the first-strand cDNA in a total
650 volume of 25 μ L. Data are the mean of three biological samples. The specificity of the
651 PCR amplification was confirmed with a heat dissociation curve (from 60°C to 95°C).
652 Efficiency of the PCR reaction was calculated and different internal standards were
653 selected (Czechowski et al., 2005) depending on the efficiency of the primers. Primers
654 used are listed in Supplemental Table S6.

655 For the gene expression analysis by RNA-seq, 21-day-old WT plants vertically grown
656 on 1/5 MS plates were used. Three independent biological replicates of WT AP and
657 roots were used for the analysis. Total RNA was extracted using NucleoSpin RNA II kit
658 (Macherey-Nagel). Using as starting material 3-15 μ g of RNA, a mRNA enrichment
659 was performed with the *MicroPoly(A) Purist kit* (AMBION). To prepare the RNA-Seq
660 library, the *SOLID Total RNA-seq* kit (Life Technologies) was used. After obtaining the
661 library, an equimolar mixture of it was used to perform an emulsion PCR using the
662 automatic system of EZ Beads (Life Technologies). Then, the bead enrichment was
663 performed followed by its deposition in the sequencing wells. The sequencing step was
664 done by SOLID 5500XL equipment of 75 nucleotides using the Exact Call Chemistry.
665 To filtrate the readings depending on their adaptor the Cutadapt v1.8 program was used.
666 FastqQC was employed to evaluate the quality of the reads. Afterward, Tophat2 was
667 employed to perform the mapping against a reference. To visualize and obtain the raw
668 counts, Seqmonk v0.29 was used.

669 **GUS activity assays and GFP microscopy**

670 GUS activity assays were performed as described in Muñoz-Bertomeu et al. (2009).
671 GFP fluorescence was observed under a confocal microscope (Leica TCS-SP). To
672 confirm the nuclear localization of PGK3, root cells were stained with 10 μ g/mL
673 Hoechst dye.

674 **Photosynthetic activity measurements**

675 Simultaneous gas exchange and chlorophyll fluorescence measurements were
676 performed as described by Faus et al. (2015). Measurements were taken 2 h after the
677 beginning of the light period to allow full photosynthesis activation.

678 **Metabolite determination and PGK activity assay**

679 The AP and roots of WT, single and double mutants, and silenced lines (two different
680 lines per silenced gene) grown on 1/5 MS plates, were used to determine metabolite
681 content in derivatized methanol extracts by GC-MS using the protocol defined in Lisec
682 et al. (2006). Metabolites were identified in comparison to database entries of authentic
683 standards (Kopka et al., 2005). Chromatograms and mass spectra were evaluated using
684 Chroma TOF 1.0 (LECO) and TagFinder 4.0 software (Luedemann et al., 2008).
685 Material was sampled for metabolite analysis after 4-6 h in the light. 3-PGA was
686 measured as previously described (Flores-Tornero et al., 2017). PGK activity was
687 measured by an enzymatic assay following NADH oxidation associated with the
688 coupled reaction of phosphoglycerate kinase and GAPDH. Frozen AP were ground in
689 liquid nitrogen and resuspended in extraction buffer (50 mM HEPES-KOH, pH 7.4, 1
690 mM EDTA, 1 mM EGTA, 2 mM Benzamidine, 2 mM E-aminocaproic acid, 0.5 mM
691 phenylmethylsulfonyl fluoride (PMSF), 10% glycerol, 0.1% Triton x-100). The

692 supernatant was obtained after centrifugation at 15000g for 20 min at 4°C. Reactions
693 were carried out in a medium containing 100 mM HEPES-KOH, 1 mM EDTA, 2 mM
694 MgSO₄, 0.3 mM NADH, 6.5 mM 3-PGA, 1 mM ATP and 3.3 Units of GAPDH. Starch
695 was determined by the ENZYTEC starch kit (ATOM) at the end of the light period.

696 **Bioinformatics and Statistics**

697 *PGK* and *TPT* genes were initially identified in the Arabidopsis Information resource.
698 The percentage of identity between different PGKs was obtained by aligning pair
699 sequences using bl2seq at NCBI (<http://blast.ncbi.nlm.nih.gov/Blast.cgi>). Amino acid
700 sequences were aligned using the ClustalOmega program
701 [<http://www.ebi.ac.uk/Tools/msa/clustalo/>; (McWilliam et al., 2013)]. Phylogenetic
702 analyses were performed according to the neighbor-joining method (Saitou and Nei,
703 1987). Units represent the number of amino acid substitutions per site for one unit. The
704 analysis was performed using the Mega6 tool (Tamura et al., 2013).

705 Experimental values represent mean values and standard error, *n* represents the number
706 of independent samples. Significant differences as compared to WT were analyzed by
707 Student's t-tests algorithms (two-tailed) using Microsoft Excel. Statistical differences
708 between groups were analyzed with a one-way ANOVA and further post hoc Tukey b
709 (WSD) test with the IBM SPSS Statistics software. The level of significance was fixed
710 at 5% (0.05).

711 **Accession numbers:**

712 Arabidopsis Genome Initiative locus identifiers of Arabidopsis genes used in this article
713 are as follows: At3g12780 (*PGK1*), At1g56190 (*PGK2*), At1g79550 (*PGK3*) and
714 At5g46110 (*TPT*).

715

716 **Acknowledgements.** We thank SCIE and UCIM of the Universitat de València for
717 technical assistance. We also thank Hellen Warburton for her language review.

718

719

720

721

Table 1. Photosynthetic parameters in *PGK* single and double mutants, and in complemented lines. Photosynthetic rate (A_N), effective (PhiPS2) and maximum photochemical yield of Photosystem II (Fv/Fm) in 20- and 30-day-old plants are shown. Each value is the mean (\pm SE) of 10 independent determinations. For each growth stage different letters indicate significant differences between groups ($P < 0.05$).

		A_N ($\mu\text{mol m}^{-2}\text{s}^{-1}$)	PhiPS2	Fv/Fm	
Mutants	20 day-old	WT	7.0 \pm 0.348 a	0.139 \pm 0.004 ab	0.769 \pm 0.003 a
		<i>pgk1.1</i>	4.7 \pm 0.332 b	0.112 \pm 0.004 c	0.745 \pm 0.008 b
		<i>pgk3.2</i>	7.5 \pm 0.408 a	0.151 \pm 0.007 a	0.766 \pm 0.006 a
		<i>pgk1.1 pgk3.2</i>	5.0 \pm 0.365 b	0.128 \pm 0.006 b	0.768 \pm 0.007 a
	30 day-old	WT	9.1 \pm 0.295 a	0.174 \pm 0.004 a	0.769 \pm 0.002 a
		<i>pgk1.1</i>	6.2 \pm 0.115 c	0.130 \pm 0.004 c	0.758 \pm 0.004 b
		<i>pgk3.2</i>	7.5 \pm 0.276 b	0.160 \pm 0.004 b	0.752 \pm 0.004 b
		<i>pgk1.1 pgk3.2</i>	7.0 \pm 0.222 b	0.140 \pm 0.004 c	0.777 \pm 0.001 a
Complemented lines	20 day-old	WT	9.0 \pm 0.606 a	0.115 \pm 0.005 a	0.778 \pm 0.003 a
		<i>pgk1.1</i>	5.1 \pm 0.502 c	0.077 \pm 0.006 c	0.748 \pm 0.005 b
		<i>pgk1.1 ProPGK1:PGK1GFP-L3</i>	7.0 \pm 0.257 b	0.089 \pm 0.004 bc	0.753 \pm 0.005 b
		<i>pgk1.1 ProPGK1:PGK1GFP-L15</i>	7.7 \pm 0.494 ab	0.101 \pm 0.006 ab	0.760 \pm 0.003 b
	30 day-old	WT	8.6 \pm 0.128 a	0.140 \pm 0.004 a	0.759 \pm 0.007 a
		<i>pgk3.2</i>	4.8 \pm 0.590 c	0.122 \pm 0.006 b	0.754 \pm 0.008 a
		<i>pgk3.2 Pro35S:PGK3-GFP-L1</i>	7.2 \pm 0.099 b	0.141 \pm 0.003 a	0.761 \pm 0.006 a
		<i>pgk3.2 Pro35S:PGK3-GFP-L11</i>	7.0 \pm 0.236 b	0.151 \pm 0.080 a	0.743 \pm 0.152 a

722

723

724 **FIGURE LEGENDS.**

725 **Figure 1.** Schematic representation of the contribution of PGKs in the primary carbon
726 metabolic pathways in photosynthetic cells. Abbreviations: 1,3-BPGA, 1,3-bis-
727 phosphoglycerate; 2-OG, 2-oxoglutarate; 2-PG, 2-phosphoglycolate; 3-PGA, 3-
728 phosphoglycerate; 3-PHP, 3-phosphohydroxypyruvate; 3-PS, 3-phosphoserine;
729 ADPGlu, ADP-glucose; AGPase, ADP-glucose pyrophosphorylase; ALD, aldolase;
730 DHAP- dihydroxyacetone phosphate; ENO, enolase; FBP, fructose 1,6-bisphosphatase;
731 Fru, fructose; Fru-1,6BP, fructose 1,6- bisphosphate; Fru-6P, fructose 6-phosphate;
732 GAP, glyceraldehyde 3-phosphate; GAPDH, glyceraldehyde 3-phosphate
733 dehydrogenase; Glu-1P, glucose 1-phosphate; Glu-6P, glucose 6-phosphate; GLYK,
734 glycerate kinase; HP, hydroxypyruvate; INV, vacuolar invertase; MEX1, maltose
735 translocator; PEP, phosphoenolpyruvate; PFK, phosphofructokinase; PGDH, 3-
736 phosphoglycerate dehydrogenase; PGI, phosphoglucoisomerase; PGK,
737 phosphoglycerate kinase; PGLm, phosphoglycerate mutase; pGluT, glucose
738 translocator; PGM, phosphoglucoisomerase; PGP, 2-phosphoglycolate phosphatase;
739 PPT, phosphoenolpyruvate translocator; PK, pyruvate kinase; PSAT, 3-phosphoserine
740 aminotransferase; PSP, 3-phosphoserine phosphatase; Ru-5P, ribulose 5-phosphate;
741 RuBP, ribulose 1,5-bisphosphate; SPP, sucrose 6-phosphate phosphatase; SPS, sucrose
742 phosphate synthase; Suc-6P, sucrose 6-phosphate; TCA, tricarboxylic acid cycle; TPI,
743 triose phosphate isomerase; TPT, triose phosphate translocator; UDPGlu, UDP-glucose;
744 UGPase, UDPGlu pyrophosphorylase;. “p” or “c” after the enzyme name denotes
745 plastidial or cytosolic isoform, respectively. Discontinuous arrows represent fluxes
746 between compartments. Hypothetical 3-PGA flux in *pgk3.2* is highlighted in red.

747

748 **Figure 2.** Expression analysis of *PGK* family genes. A and B, RT-PCR analysis of
749 *PGKs* in 18-day-old seedlings grown in a MS 1/5 medium (A) and in adult plants grown
750 under greenhouse conditions (B). C, *GUS* expression under the control of *PGK1*, *PGK2*
751 and the *PGK3* promoter in different plant organs. Scale Bars = 1 mm (cotyledons,
752 leaves and flowers), 0.1 mm (roots). Values in A and B (mean \pm SE; n = 3 independent
753 biological replicates) are normalized to the expression in the Aerial parts (A) or stems
754 (B).

755

756 **Figure 3.** Subcellular localization of PGK isoforms by stable expression of PGK-GFP
757 fusion proteins under the control of PGK native promoters. Bars = 100 μ m.

758 **Figure 4.** Genomic organization and expression analysis of the *PGK* and *TPT* T-DNA
759 mutant lines. A, Black boxes represent exons and grey lines introns. The T-DNA
760 insertion point in each mutant is shown. B, Detection of the *PGK* and *TPT* transcripts in
761 the aerial parts of 18-day-old seedlings of single and double mutants by RT-PCR
762 analysis. Values (mean \pm SE; n = 3 independent biological replicates) are normalized to
763 the expression in the wild-type (WT).

764

765 **Figure 5.** Phenotypical analysis of *PGK* T-DNA mutants and silenced lines grown in
766 MS 1/5 (18-day-old seedlings) or greenhouse conditions (30-day-old plants) as
767 compared to wild-type plants (WT). Seedling aerial part (AP) and root fresh weight
768 (FW) of different lines grown in vertical plates are shown in A and B, respectively.
769 Rosette FW is shown in C. D, picture of a representative individual of each line grown
770 in greenhouse. E, FW of the AP of mutant and the complemented lines grown in

771 greenhouse. Values are the mean \pm SE ($n \geq 36$ plants). In (E) data are the mean of two
772 independent transgenic lines. * Significantly different as compared to WT; different
773 letters indicate significant differences between WT, single and double mutants ($P <$
774 0.05).
775

776 **Figure 6.** Biochemical and molecular analyses of *PGK* mutant and silenced lines
777 (amiRNA lines) as compared to wild-type plants (WT). A, B, and C, starch content,
778 *PGK* activity and RT-PCR analysis of *PGKs* in the aerial parts (AP) of 20- and 30-day-
779 old plants grown in greenhouse. In B, *PGK* activity was also measured in 20-day-old
780 roots grown in plates. Values are the mean \pm SE ($n \geq 30$ plants). In A and B, data from
781 the silenced lines are the mean of individuals from two independent transgenic lines. *
782 Significantly different as compared to the WT; different letters indicate significant
783 differences between groups ($P < 0.05$).

784 **Figure 7.** Most relevant changes in the metabolite content of aerial parts (AP) and roots
785 of 21-day-old *pgk* mutants and silenced lines grown in vertical plates as compared to
786 wild-type (WT). Log^2 values of the relative metabolic contents are presented as a heat-
787 map. *Significant differences between the mutant and the wild type (WT) ($P < 0.05$).
788 Detailed results of the assay are presented in Supplemental Tables S3 and S4.

789 **Figure 8.** Phenotypical, biochemical and molecular analyses of *pgk3.2 tpt3* mutant as
790 compared to single mutants (*pgk3.2*, *tpt3*) and wild-type (WT). A, relative 3-PGA
791 content in the aerial parts (AP) of 25-day-old plants grown in greenhouse normalized to
792 the mean content of the WT ($34 \pm 1 \mu\text{g g}^{-1}$ fresh weight). B and C, Rosette fresh weight
793 (FW) and starch content of the AP of 25-day-old plants grown in greenhouse. D, most
794 relevant changes in the metabolite content of AP of 19-day-old *pgk3.2 tpt3* lines grown
795 in vertical plates as compared to single mutants and wild-type (WT). Log^2 values of the
796 relative metabolic contents are presented as a heat-map. Detailed results of the assay are
797 presented in Supplemental Table S5. * Significantly different as compared to WT;
798 different letters indicate significant differences between groups ($P < 0.05$).
799

800

801 **SUPPLEMENTAL MATERIAL**

802 **Supplemental Figure S1.** Amino acid alignment and cladogram of the Arabidopsis
803 PGK proteins.

804 **Supplemental Figure S2.** Expression of GUS under the control of *PGK1* promoter in
805 seedlings and adult plants.

806 **Supplemental Figure S3.** Expression of GUS under the control of *PGK2* promoter in
807 seedlings and adult plants.

808 **Supplemental Figure S4.** *GUS* Expression under the control of *PGK3* promoter in
809 seedlings and adult plants.

810 **Supplemental Figure S5.** Subcellular localization of PGK3 by stable expression of
811 PGK-GFP fusion proteins under the control of *35S* promoter.

812 **Supplemental Figure S6.** RT-PCR analysis of the aerial parts of 20-day-old seedlings
813 of *PGK2* (A) and *PGK1* (B) silenced lines grown on vertical plates.

814 **Supplemental Table S1.** Genomic localization of *PGK* family T-DNA mutant lines
815 confirmed by sequencing.

816 **Supplemental Table S2.** Photosynthetic parameters in wild-type (WT) and two
817 independent amiPGK2 silenced lines (*amiPGK2-H35*, *amiPGK2-H49*).

818 **Supplemental Table S3.** Metabolite levels in the aerial parts of 21-day-old *PGK* single
819 (*pgk1.1*, *pgk3.2*) and double (*pgk1.1 pgk3.2*) mutants, silenced (*amiPGK2*) lines, and
820 wild-type (WT).

821 **Supplemental Table S4.** Metabolite levels in the roots of 21-day-old *PGK* single
822 (*pgk1.1*, *pgk3.2*) and double (*pgk1.1 pgk3.2*) mutants, silenced (*amiPGK2*) lines, and
823 wild-type (WT).

824 **Supplemental Table S5.** Metabolite levels in the aerial parts of 19-day-old *PGK3* and
825 *TPT* single (*pgk3.2*, *tpt3*) and double (*pgk3.2 tpt3*) mutants, and wild-type (WT) plants.

826 **Supplemental Table S6.** List of primers used in this work.

827

828

829

830 **Supplemental Figure S1.** Amino acid alignment and cladogram of the Arabidopsis
831 PGK proteins. A, Amino acid alignment of Arabidopsis PGK family proteins using the
832 ClustalOmega program. Asterisks denote the same amino acid between sequences, a
833 colon indicates conserved amino acids. Amino acids that form the ligand binding
834 domain are marked with empty triangles, the ADP binding domain with black triangles,
835 and the catalytic site is marked with grey triangles. B, The phylogenetic tree was
836 constructed from an alignment of the deduced amino acid sequences, as described in
837 Materials and Methods (M&M). Branch length is given under each segment according
838 to the algorithm specified in M&M.

839 **Supplemental Figure S2.** Expression of GUS under the control of *PGK1* promoter in
840 seedlings and adult plants. Cotyledon (A), Leaves (B), Stomata (C), Hypocotyl (D),
841 Roots (E, F), Caulin leaves (G, H), Rosette leaves (I), Flowers (J), Siliques (K), Roots
842 (L). Bars = 1 mm (A, B, D, G, J, K), 0.5 mm (F, L), 0.2 mm (H,J) and 0.1 mm (C, E).

843

844 **Supplemental Figure S3.** Expression of GUS under the control of *PGK2* promoter in
845 seedlings and adult plants. Cotyledon (A), Leaves (B), Stomata (C), Roots (D), Rosette
846 leaves (E), Flowers (F), Stigma (G), Anthers and stigma (H), Siliques (I) and Roots (J).
847 Bars = 1 mm (A, B, E, F, H, I), 0.5 mm (G), 0.2 mm (D) and 0.1 mm (C, J).

848

849 **Supplemental Figure S4.** *GUS* Expression under the control of *PGK3* promoter in
850 seedlings and adult plants. Cotyledon (A), Leaves (B), Roots (C), Rosette leaves (D, E),
851 Siliques (F), Flowers (G), Anther (H) and Roots (I). Bars = 1 mm (A, B, D, E, F, G), 0.5
852 mm (H, I) and 0.1 mm (C).

853

854 **Supplemental Figure S5.** Subcellular localization of PGK3 by stable expression of
855 PGK-GFP fusion proteins under the control of 35S promoter. The nuclear localization
856 of PGK3 was visualized by staining root cells with the Hoechst marker. Bar = 10 μ m.

857

858

859 **Supplemental Figure S6.** RT-PCR analysis of the aerial parts of 20-day-old seedlings
860 of *PGK2* (A) and *PGK1* (B) silenced lines grown on vertical plates.

861 **Supplemental Table S1.** Genomic localization of *PGK* family T-DNA mutant lines
862 confirmed by sequencing. Nucleotide numbering is relative to the gene translation start
863 codon.

864 **Supplemental Table S2.** Photosynthetic parameters in wild-type (WT) and two
865 independent amiPGK2 silenced lines (*amiPGK2-H35*, *amiPGK2-H49*). Photosynthetic
866 rate (A_N), effective (PhiPS2) and maximum photochemical yield of Photosystem II
867 (Fv/Fm) were determined in 20-day-old plants. Each value is the mean (\pm SE) of 10
868 independent determinations. ns, indicates non-significant differences between groups (P
869 < 0.05).

870

871 **Supplemental Table S3.** Metabolite levels in the aerial parts of 21-day-old *PGK* single
872 (*pgk1.1*, *pgk3.2*) and double (*pgk1.1 pgk3.2*) mutants, silenced (*amiPGK2*) lines, and
873 wild-type (WT). Data are relative values normalized to the mean response calculated for
874 each WT. Values represent the mean \pm SE of six independent determinations for WT
875 and *PGK* mutants, and 12 determinations for *amiPGK2* (corresponding to samples of
876 two independent transgenic plants). Those values that were significantly different to WT
877 are set in bold type, $P < 0.05$. ND, Non detected.

878 **Supplemental Table S4.** Metabolite levels in the roots of 21-day-old *PGK* single
879 (*pgk1.1*, *pgk3.2*) and double (*pgk1.1 pgk3.2*) mutants, silenced (*amiPGK2*) lines, and
880 wild-type (WT). Data are relative values normalized to the mean response calculated for
881 each WT. Values represent the mean \pm SE of six independent determinations for WT
882 and *PGK* mutants, and 12 determinations for *amiPGK2* (corresponding to samples of
883 two independent transgenic plants). Those values that were significantly different to WT
884 are set in bold type, $P < 0.05$. ND, Non detected.

885 **Supplemental Table S5.** Metabolite levels in the aerial parts of 19-day-old *PGK3* and
886 *TPT* single (*pgk3.2*, *tpt3*) and double (*pgk3.2 tpt3*) mutants, and wild-type (WT) plants.
887 Data are relative values normalized to the mean response calculated for each WT.
888 Values represent the mean \pm SE of six independent determinations. Those values that
889 are significantly different to WT are set in bold type, $P < 0.05$.

890

891 **Supplemental Table S6.** List of primers used in this work.

892

894 LITERATURE CITED

- 895 **Ai J, Huang H, Lv X, Tang Z, Chen M, Chen T, Duan W, Sun H, Li Q, Tan R, Liu**
 896 **Y, Duan J, Yang Y, Wei Y, Li Y, Zhou Q** (2011) FLNA and PGK1 are two
 897 potential markers for progression in hepatocellular carcinoma. *Cell Physiol*
 898 *Biochem* **27**: 207-216
- 899 **Alonso JM, Stepanova AN, Leisse TJ, Kim CJ, Chen H, Shinn P, Stevenson DK,**
 900 **Zimmerman J, Barajas P, Cheuk R, Gadrinab C, Heller C, Jeske A,**
 901 **Koesema E, Meyers CC, Parker H, Prednis L, Ansari Y, Choy N, Deen H,**
 902 **Geralt M, Hazari N, Hom E, Karnes M, Mulholland C, Ndubaku R,**
 903 **Schmidt I, Guzman P, Aguilar-Henonin L, Schmid M, Weigel D, Carter**
 904 **DE, Marchand T, Risseuw E, Brogden D, Zeko A, Crosby WL, Berry CC,**
 905 **Ecker JR** (2003) Genome-wide insertional mutagenesis of *Arabidopsis*
 906 *thaliana*. *Science* **301**: 653-657
- 907 **Anderson LE, Advani VR** (1970) Chloroplast and cytoplasmic enzymes: three distinct
 908 isoenzymes associated with the reductive pentose phosphate cycle. *Plant Physiol*
 909 **45**: 583-585
- 910 **Anderson LE, Bryant JA, Carol AA** (2004) Both chloroplastic and cytosolic
 911 phosphoglycerate kinase isozymes are present in the pea leaf nucleus.
 912 *Protoplasma* **223**: 103-110
- 913 **Anoman AD, Muñoz-Bertomeu J, Rosa-Téllez S, Flores-Tornero M, Serrano R,**
 914 **Bueso E, Fernie AR, Segura J, Ros R** (2015) Plastidial glycolytic
 915 glyceraldehyde-3-phosphate dehydrogenase is an important determinant in the
 916 carbon and nitrogen metabolism of heterotrophic cells in *Arabidopsis*. *Plant*
 917 *Physiol* **169**: 1619-1637
- 918 **Archibald JM, Keeling PJ** (2003) Comparative genomics. Plant genomes:
 919 cyanobacterial genes revealed. *Heredity* **90**: 2-3
- 920 **Blasing OE, Gibon Y, Gunther M, Hohne M, Morcuende R, Osuna D, Thimm O,**
 921 **Usadel B, Scheible WR, Stitt M** (2005) Sugars and circadian regulation make
 922 major contributions to the global regulation of diurnal gene expression in
 923 *Arabidopsis*. *Plant Cell* **17**: 3257-3281
- 924 **Boer PH, Adra CN, Lau YF, McBurney MW** (1987) The testis-specific
 925 phosphoglycerate kinase gene *pgk-2* is a recruited retroposon. *Mol Cell Biol* **7**:
 926 3107-3112
- 927 **Brice DC, Bryant JA, Dambrauskas G, Drury SC, Littlechild JA** (2004) Cloning
 928 and expression of cytosolic phosphoglycerate kinase from pea (*Pisum sativum*
 929 L.). *J Exp Bot* **55**: 955-956
- 930 **Brinkmann H, Martin W** (1996) Higher-plant chloroplast and cytosolic 3-
 931 phosphoglycerate kinases: a case of endosymbiotic gene replacement. *Plant Mol*
 932 *Biol* **30**: 65-75
- 933 **Cascales-Miñana B, Muñoz-Bertomeu J, Flores-Tornero M, Anoman AD, Pertusa**
 934 **J, Alaiz M, Osorio S, Fernie AR, Segura J, Ros R** (2013) The phosphorylated
 935 pathway of serine biosynthesis is essential both for malegametophyte and
 936 embryo development and for root growth in *Arabidopsis*. *Plant Cell* **25**: 2084-
 937 2101
- 938 **Clough SJ, Bent AF** (1998) Floral dip: a simplified method for *Agrobacterium*-
 939 mediated transformation of *Arabidopsis thaliana*. *Plant J* **16**: 735-743
- 940 **Curtis MD, Grossniklaus U** (2003) A gateway cloning vector set for high-throughput
 941 functional analysis of genes in planta. *Plant Physiol* **133**: 462-469

- 942 **Chen M, Thelen JJ** (2010) The plastid isoform of triose phosphate isomerase is
943 required for the postgerminative transition from heterotrophic to autotrophic
944 growth in *Arabidopsis*. *Plant Cell* **22**: 77-90
- 945 **Cheng SF, Huang YP, Chen LH, Hsu YH, Tsai CH** (2013) Chloroplast
946 phosphoglycerate kinase is involved in the targeting of *Bamboo mosaic virus* to
947 chloroplasts in *Nicotiana benthamiana* plants. *Plant Physiol* **163**: 1598-1608
- 948 **Chiarelli LR, Morera SM, Bianchi P, Fermo E, Zanella A, Galizzi A, Valentini G**
949 (2012) Molecular insights on pathogenic effects of mutations causing
950 phosphoglycerate kinase deficiency. *PLoS One* **7**: e32065
- 951 **Czechowski T, Stitt M, Altmann T, Udvardi MK, Scheible WR** (2005) Genome-
952 wide identification and testing of superior reference genes for transcript
953 normalization in *Arabidopsis*. *Plant Physiol* **139**: 5-17
- 954 **Danshina PV, Geyer CB, Dai Q, Goulding EH, Willis WD, Kitto GB, McCarrey
955 JR, Eddy EM, O'Brien DA** (2010) Phosphoglycerate kinase 2 (PGK2) is
956 essential for sperm function and male fertility in mice. *Biol Reprod* **82**: 136-145
- 957 **Emanuelsson O, Nielsen H, von Heijne G** (1999) ChloroP, a neural network-based
958 method for predicting chloroplast transit peptides and their cleavage sites.
959 *Protein Sci* **8**: 978-984
- 960 **Faus I, Zabalza A, Santiago J, Nebauer SG, Royuela M, Serrano R, Gadea J** (2015)
961 Protein kinase GCN2 mediates responses to glyphosate in *Arabidopsis*. *BMC*
962 *Plant Biol* **15**: 14
- 963 **Fermani S, Sparla F, Falini G, Martelli PL, Casadio R, Pupillo P, Ripamonti A,
964 Trost P** (2007) Molecular mechanism of thioredoxin regulation in
965 photosynthetic A2B2-glyceraldehyde-3-phosphate dehydrogenase. *Proc Natl
966 Acad Sci USA* **104**: 11109-11114
- 967 **Fischer K, Weber A** (2002) Transport of carbon in non-green plastids. *Trends Plant Sci*
968 **7**: 345-351
- 969 **Flores-Tornero M, Anoman AD, Rosa-Téllez S, Toujani W, Weber AP, Eisenhut
970 M, Kurz S, Alseekh S, Fernie AR, Muñoz-Bertomeu J, Ros R** (2017)
971 Overexpression of the triose phosphate translocator (TPT) complements the
972 abnormal metabolism and development of plastidial glycolytic glyceraldehyde-
973 3-phosphate dehydrogenase mutants. *Plant J* **89**: 1146-1158
- 974 **Guo L, Devaiah SP, Narasimhan R, Pan X, Zhang Y, Zhang W, Wang X** (2012)
975 Cytosolic glyceraldehyde-3-phosphate dehydrogenases interact with
976 phospholipase D δ to transduce hydrogen peroxide signals in the *Arabidopsis*
977 response to stress. *Plant Cell* **24**: 2200-2212
- 978 **Guo L, Ma F, Wei F, Fanella B, Allen DK, Wang X** (2014) Cytosolic
979 phosphorylating glyceraldehyde-3-phosphate dehydrogenases affect *Arabidopsis*
980 cellular metabolism and promote seed oil accumulation. *Plant Cell* **26**: 3023-
981 3035
- 982 **Hajirezaei MR, Biemelt S, Peisker M, Lytovchenko A, Fernie AR, Sonnewald U**
983 (2006) The influence of cytosolic phosphorylating glyceraldehyde 3-phosphate
984 dehydrogenase (GAPC) on potato tuber metabolism. *J Exp Bot* **57**: 2363-2377
- 985 **Han S, Wang Y, Zheng X, Jia Q, Zhao J, Bai F, Hong Y, Liu Y** (2015) Cytoplasmic
986 glyceraldehyde-3-phosphate dehydrogenases interact with ATG3 to negatively
987 regulate autophagy and immunity in *Nicotiana benthamiana*. *Plant Cell* **27**:
988 1316-1331
- 989 **Holtgreve S, Gohlke J, Starmann J, Druce S, Klocke S, Altmann B, Wojtera J,
990 Lindermayr C, Scheibe R** (2008) Regulation of plant cytosolic glyceraldehyde

991 3-phosphate dehydrogenase isoforms by thiol modifications. *Physiol Plant* **133**:
992 211-228

993 **Hwang TL, Liang Y, Chien KY, Yu JS** (2006) Overexpression and elevated serum
994 levels of phosphoglycerate kinase 1 in pancreatic ductal adenocarcinoma.
995 *Proteomics* **6**: 2259-2272

996 **Joshi R, Karan R, Singla-Pareek SL, Pareek A** (2016) Ectopic expression of Pokkali
997 phosphoglycerate kinase-2 (OsPGK2-P) improves yield in tobacco plants under
998 salinity stress. *Plant Cell Rep* **35**: 27-41

999 **Kopka J, Schauer N, Krueger S, Birkemeyer C, Usadel B, Bergmuller E, Dormann**
1000 **P, Weckwerth W, Gibon Y, Stitt M, Willmitzer L, Fernie AR, Steinhauser**
1001 **D** (2005) GMD@CSB.DB: the Golm Metabolome Database. *Bioinformatics* **21**:
1002 1635-1638

1003 **Köpke-Secundo E, Molnar I, Schnarrenberger C** (1990) Isolation and
1004 characterization of the cytosolic and chloroplastic 3-phosphoglycerate kinase
1005 from spinach leaves. *Plant Physiol* **93**: 40-47

1006 **Krietsch WK, Bucher T** (1970) 3-phosphoglycerate kinase from rabbit skeletal muscle
1007 and yeast. *Eur J Biochem* **17**: 568-580

1008 **Lay AJ, Jiang XM, Kisker O, Flynn E, Underwood A, Condrón R, Hogg PJ** (2000)
1009 Phosphoglycerate kinase acts in tumour angiogenesis as a disulphide reductase.
1010 *Nature* **408**: 869-873

1011 **Lin JW, Ding MP, Hsu YH, Tsai CH** (2007) Chloroplast phosphoglycerate kinase, a
1012 gluconeogenic enzyme, is required for efficient accumulation of *Bamboo*
1013 *mosaic virus*. *Nucleic Acids Res* **35**: 424-432

1014 **Lisec J, Schauer N, Kopka J, Willmitzer L, Fernie AR** (2006) Gas chromatography
1015 mass spectrometry-based metabolite profiling in plants. *Nat Protoc* **1**: 387-396

1016 **Liu D, Li W, Cheng J, Hou L** (2015) *AtPGK2*, a member of PGKs gene family in
1017 *Arabidopsis*, has a positive role in salt stress tolerance. *Plant Cell Tissue Organ*
1018 *Culture* **120**: 251-262

1019 **Lobler M** (1998) Two phosphoglycerate kinase cDNAs from *Arabidopsis thaliana*.
1020 *DNA Sequence* **8**: 247-252

1021 **Longstaff M, Raines CA, McMorrow EM, Bradbeer JW, Dyer TA** (1989) Wheat
1022 phosphoglycerate kinase: evidence for recombination between the genes for the
1023 chloroplastic and cytosolic enzymes. *Nucleic Acids Res* **17**: 6569-6580

1024 **Luedemann A, Strassburg K, Erban A, Kopka J** (2008) TagFinder for the
1025 quantitative analysis of gas chromatography–mass spectrometry (GC-MS)-based
1026 metabolite profiling experiments. *Bioinformatics* **24**: 732-737

1027 **McCarrey JR, Thomas K** (1987) Human testis-specific PGK gene lacks introns and
1028 possesses characteristics of a processed gene. *Nature* **326**: 501-505

1029 **McCormick AJ, Kruger NJ** (2015) Lack of fructose 2,6-bisphosphate compromises
1030 photosynthesis and growth in *Arabidopsis* in fluctuating environments. *Plant J*
1031 **81**: 670-683

1032 **McMorrow EM, Bradbeer JW** (1990) Separation, purification, and comparative
1033 properties of chloroplast and cytoplasmic phosphoglycerate kinase from barley
1034 leaves. *Plant Physiol* **93**: 374-383

1035 **McWilliam H, Li W, Uludag M, Squizzato S, Park YM, Buso N, Cowley AP, Lopez**
1036 **R** (2013) Analysis Tool Web Services from the EMBL-EBI. *Nucleic Acids Res*
1037 **41**: W597-W600

1038 **Morisse S, Michelet L, Bedhomme M, Marchand CH, Calvaresi M, Trost P,**
1039 **Fermani S, Zaffagnini M, Lemaire SD** (2014) Thioredoxin-dependent redox

- 1040 regulation of chloroplastic phosphoglycerate kinase from *Chlamydomonas*
1041 *reinhardtii*. J Biol Chem **289**: 30012-30024
- 1042 **Muñoz-Bertomeu J, Cascales-Miñana B, Irlles-Segura A, Mateu I, Nunes-Nesi A,**
1043 **Fernie AR, Segura J, Ros R** (2010) The plastidial glyceraldehyde-3-phosphate
1044 dehydrogenase is critical for viable pollen development in Arabidopsis. Plant
1045 Physiol **152**: 1830-1841
- 1046 **Muñoz-Bertomeu J, Cascales-Miñana B, Mulet JM, Baroja-Fernandez E, Pozueta-**
1047 **Romero J, Kuhn JM, Segura J, Ros R** (2009) Plastidial glyceraldehyde-3-
1048 phosphate dehydrogenase deficiency leads to altered root development and
1049 affects the sugar and amino acid balance in Arabidopsis. Plant Physiol **151**: 541-
1050 558
- 1051 **Myouga F, Akiyama K, Motohashi R, Kuromori T, Ito T, Iizumi H, Ryusui R,**
1052 **Sakurai T, Shinozaki K** (2010) The Chloroplast Function Database: a large-
1053 scale collection of Arabidopsis *Ds/Spm*- or T-DNA-tagged homozygous lines for
1054 nuclear-encoded chloroplast proteins, and their systematic phenotype analysis.
1055 Plant J **61**: 529-542
- 1056 **Ouibrahim L, Mazier M, Estevan J, Pagny G, Decroocq V, Desbiez C, Moretti A,**
1057 **Gallois JL, Caranta C** (2014) Cloning of the Arabidopsis *rwm1* gene for
1058 resistance to *Watermelon mosaic virus* points to a new function for natural virus
1059 resistance genes. Plant J **79**: 705-716
- 1060 **Paul MJ, Pellny TK** (2003) Carbon metabolite feedback regulation of leaf
1061 photosynthesis and development. J Exp Bot **54**: 539-547
- 1062 **Petersen J, Brinkmann H, Cerff R** (2003) Origin, evolution, and metabolic role of a
1063 novel glycolytic GAPDH enzyme recruited by land plant plastids. J Mol Evol
1064 **57**: 16-26
- 1065 **Plaxton WC** (1996) The organization and regulation of plant glycolysis. Annu Rev
1066 Plant Physiol Plant Mol Biol **47**: 185-214
- 1067 **Popanda O, Fox G, Thielmann HW** (1998) Modulation of DNA polymerases α , δ and
1068 ϵ by lactate dehydrogenase and 3-phosphoglycerate kinase. Biochim Biophys
1069 Acta **1397**: 102-117
- 1070 **Prabhakar V, Lottgert T, Geimer S, Dormann P, Kruger S, Vijayakumar V,**
1071 **Schreiber L, Gobel C, Feussner K, Feussner I, Marin K, Staehr P, Bell K,**
1072 **Flugge UI, Hausler RE** (2010) Phosphoenolpyruvate provision to plastids is
1073 essential for gametophyte and sporophyte development in *Arabidopsis thaliana*.
1074 Plant Cell **22**: 2594-2617
- 1075 **Rius SP, Casati P, Iglesias AA, Gomez-Casati DF** (2006) Characterization of an
1076 *Arabidopsis thaliana* mutant lacking a cytosolic non-phosphorylating
1077 glyceraldehyde-3-phosphate dehydrogenase. Plant Mol Biol **61**: 945-957
- 1078 **Saitou N, Nei M** (1987) The neighbor-joining method: a new method for reconstructing
1079 phylogenetic trees. Mol Biol Evol **4**: 406-425
- 1080 **Sambrook J, Russell DW** (2001) Molecular cloning: A laboratory manual, Ed 3. Cold
1081 Spring Harbor Laboratory Press, Cold Spring Harbor, NY
- 1082 **Scholl RL, May ST, Ware DH** (2000) Seed and molecular resources for Arabidopsis.
1083 Plant Physiol **124**: 1477-1480
- 1084 **Shih MC, Lazar G, Goodman HM** (1986) Evidence in favor of the symbiotic origin of
1085 chloroplasts: primary structure and evolution of tobacco glyceraldehyde-3-
1086 phosphate dehydrogenases. Cell **47**: 73-80
- 1087 **Smith AM, Stitt M** (2007) Coordination of carbon supply and plant growth. Plant Cell
1088 Environ **30**: 1126-1149

1089 **Sparla F, Zaffagnini M, Wedel N, Scheibe R, Pupillo P, Trost P** (2005) Regulation
1090 of photosynthetic GAPDH dissected by mutants. *Plant Physiol* **138**: 2210-2219

1091 **Staehr P, Lottgert T, Christmann A, Krueger S, Rosar C, Rolcik J, Novak O,**
1092 **Strnad M, Bell K, Weber AP, Flugge UI, Hausler RE** (2014) Reticulate
1093 leaves and stunted roots are independent phenotypes pointing at opposite roles
1094 of the phosphoenolpyruvate/phosphate translocator defective in *cuel* in the
1095 plastids of both organs. *Front Plant Sci* **5**: 1-5

1096 **Stitt M, Lunn J, Usadel B** (2010) Arabidopsis and primary photosynthetic metabolism
1097 - more than the icing on the cake. *Plant J* **61**: 1067-1091

1098 **Tamura K, Stecher G, Peterson D, Filipinski A, Kumar S** (2013) MEGA6: Molecular
1099 Evolutionary Genetics Analysis version 6.0. *Mol Biol Evol* **30**: 2725-2729

1100 **Troncoso-Ponce MA, Garces R, Martinez-Force E** (2010) Glycolytic enzymatic
1101 activities in developing seeds involved in the differences between standard and
1102 low oil content sunflowers (*Helianthus annuus* L.). *Plant Physiol Biochem* **48**:
1103 961-965

1104 **Troncoso-Ponce MA, Kruger NJ, Ratcliffe G, Garces R, Martinez-Force E** (2009)
1105 Characterization of glycolytic initial metabolites and enzyme activities in
1106 developing sunflower (*Helianthus annuus* L.) seeds. *Phytochemistry* **70**: 1117-
1107 1122

1108 **Troncoso-Ponce MA, Rivoal J, Venegas-Caleron M, Dorion S, Sanchez R, Cejudo**
1109 **FJ, Garces R, Martinez-Force E** (2012) Molecular cloning and biochemical
1110 characterization of three phosphoglycerate kinase isoforms from developing
1111 sunflower (*Helianthus annuus* L.) seeds. *Phytochemistry* **79**: 27-38

1112 **Wakao S, Chin BL, Ledford HK, Dent RM, Casero D, Pellegrini M, Merchant SS,**
1113 **Niyogi KK** (2014) Phosphoprotein SAK1 is a regulator of acclimation to singlet
1114 oxygen in *Chlamydomonas reinhardtii*. *Elife* **3**: e02286

1115 **Willard HF, Goss SJ, Holmes MT, Munroe DL** (1985) Regional localization of the
1116 phosphoglycerate kinase gene and pseudogene on the human X chromosome
1117 and assignment of a related DNA sequence to chromosome 19. *Hum Genet* **71**:
1118 138-143

1119 **Zhao Z, Assmann SM** (2011) The glycolytic enzyme, phosphoglycerate mutase, has
1120 critical roles in stomatal movement, vegetative growth, and pollen production in
1121 *Arabidopsis thaliana*. *J Exp Bot* **62**: 5179-5189

1122 **Zieker D, Konigsrainer I, Traub F, Nieselt K, Knapp B, Schillinger C, Stirnkorb**
1123 **C, Fend F, Northoff H, Kupka S, Brucher BL, Konigsrainer A** (2008) PGK1
1124 a potential marker for peritoneal dissemination in gastric cancer. *Cell Physiol*
1125 *Biochem* **21**: 429-436

1126 **Zieker D, Konigsrainer I, Weinreich J, Beckert S, Glatzle J, Nieselt K, Buhler S,**
1127 **Loffler M, Gaedcke J, Northoff H, Mannheim JG, Wiehr S, Pichler BJ, von**
1128 **Weyhern C, Brucher BL, Konigsrainer A** (2010) Phosphoglycerate kinase 1
1129 promoting tumor progression and metastasis in gastric cancer - detected in a
1130 tumor mouse model using positron emission tomography/magnetic resonance
1131 imaging. *Cell Physiol Biochem* **26**: 147-154

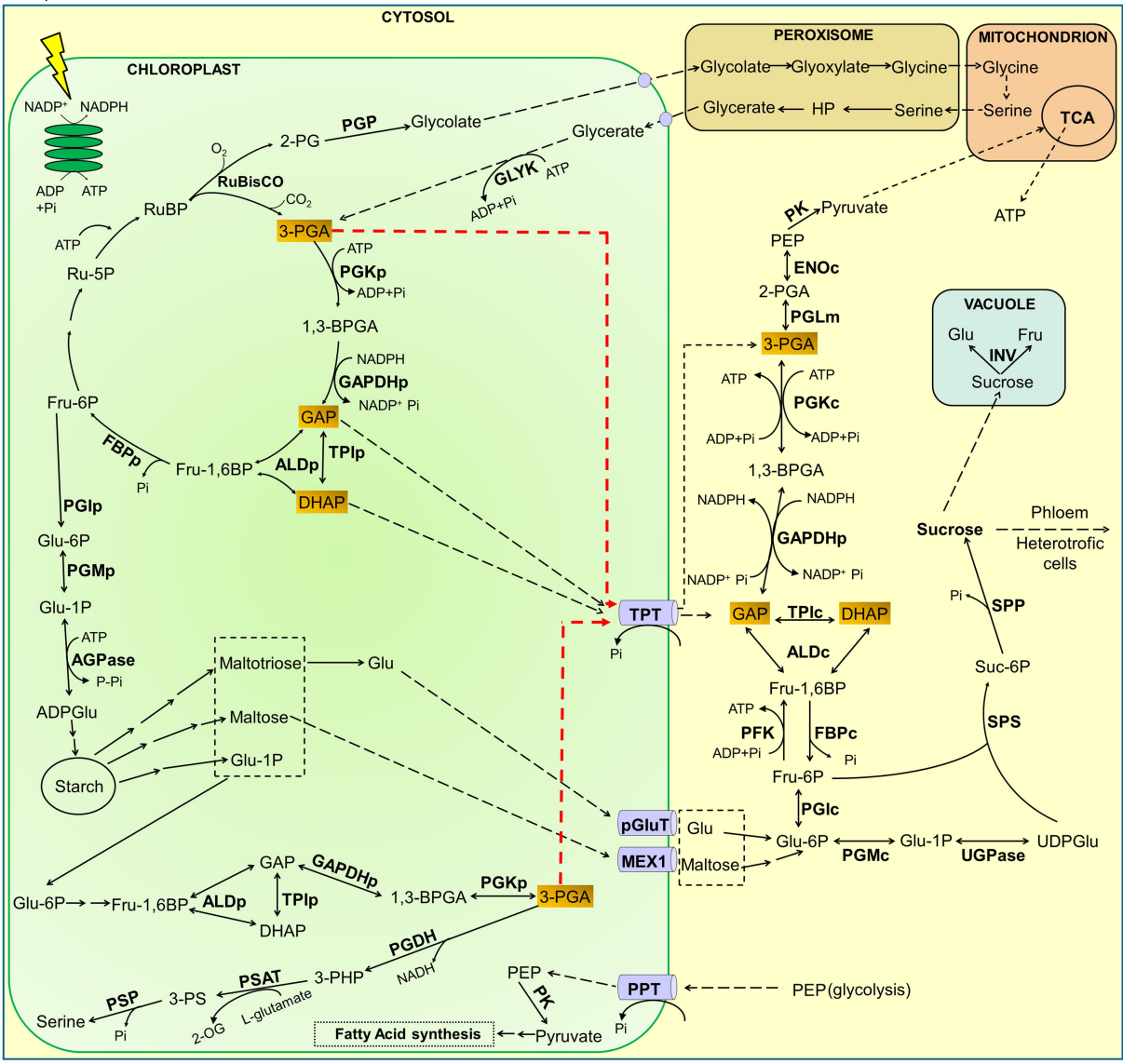
1132

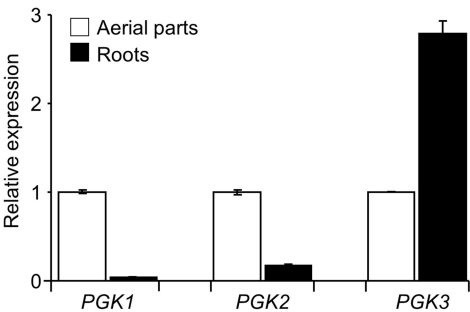
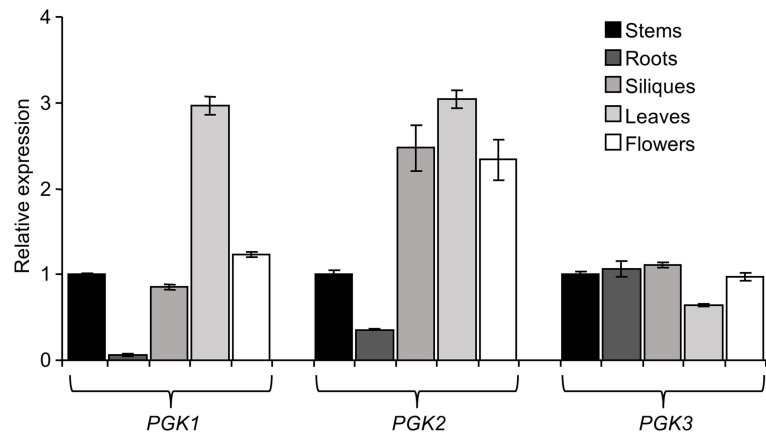
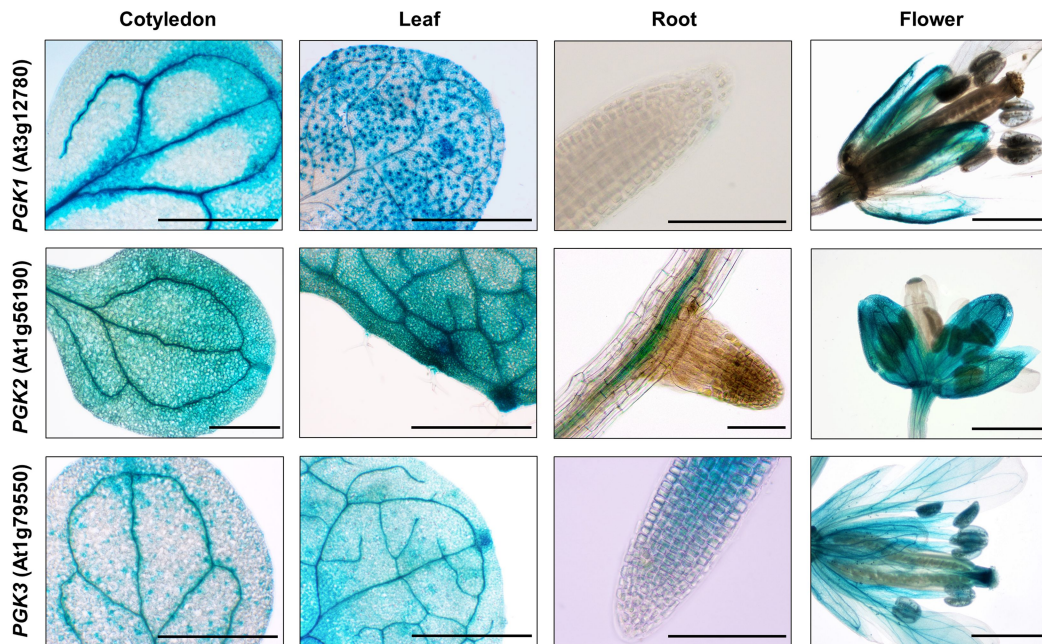
1133

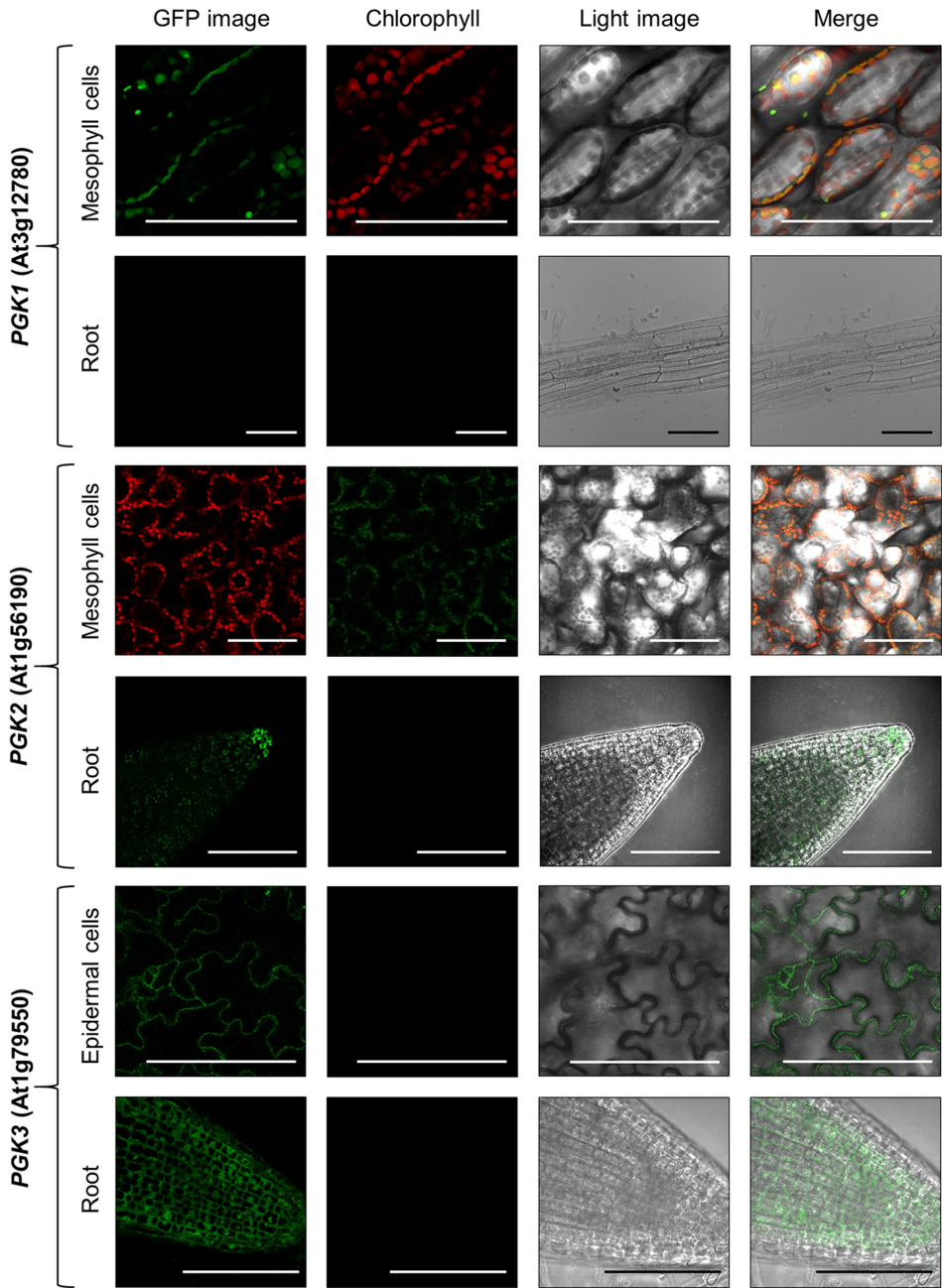
1134

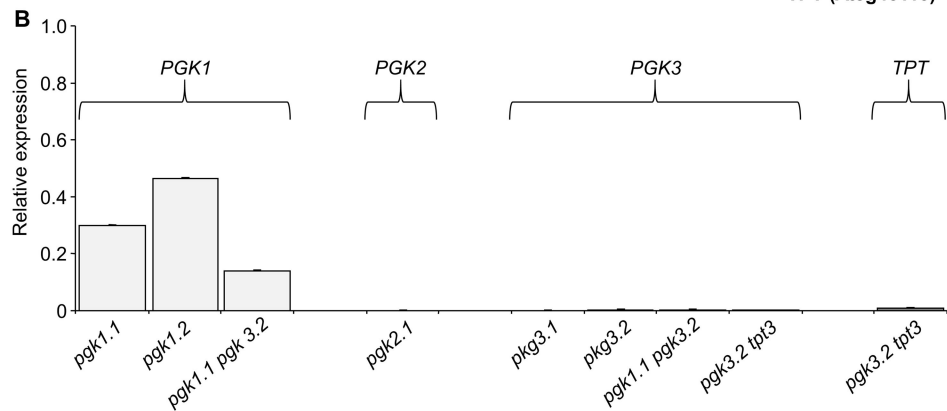
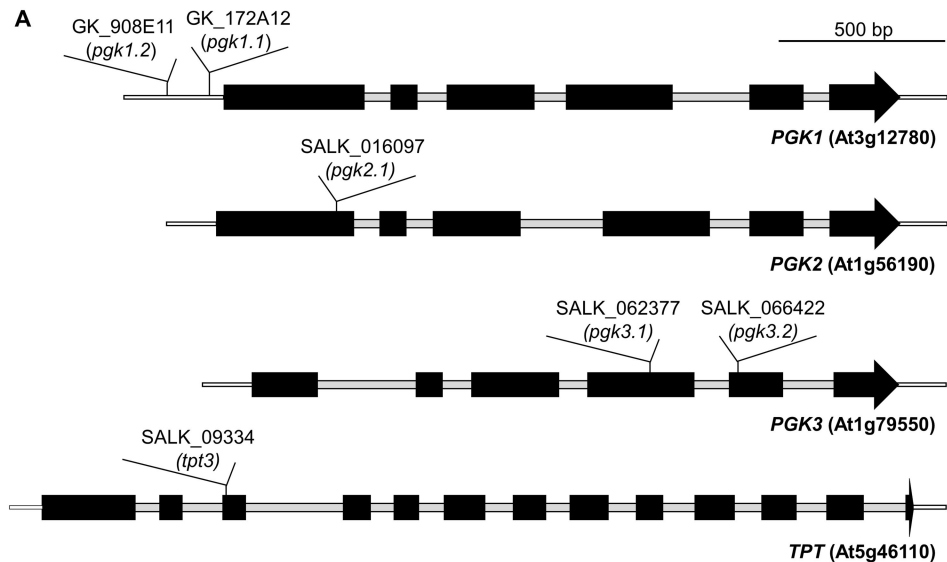
1135

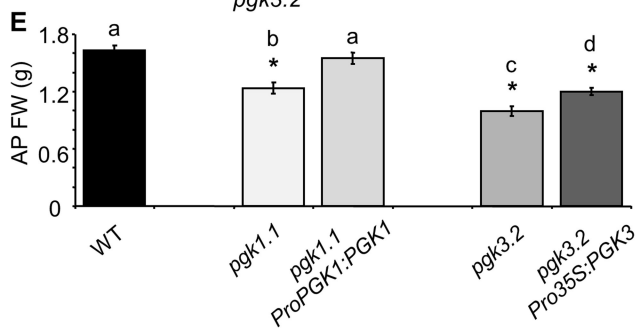
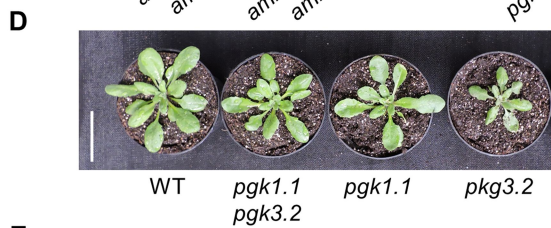
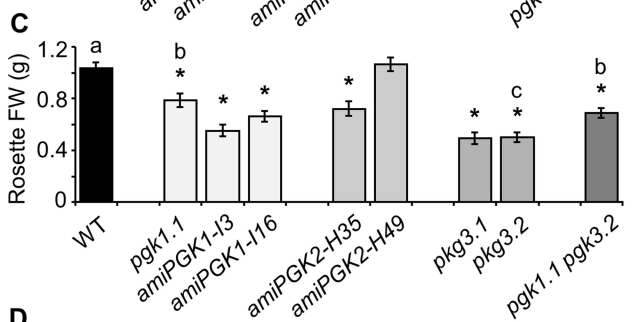
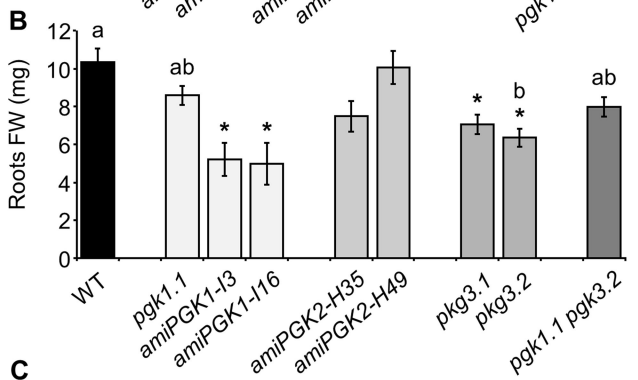
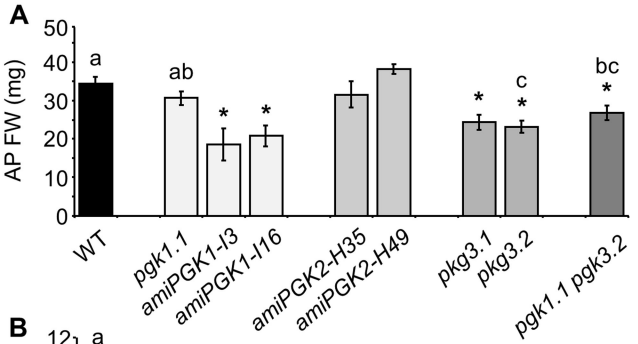
1136

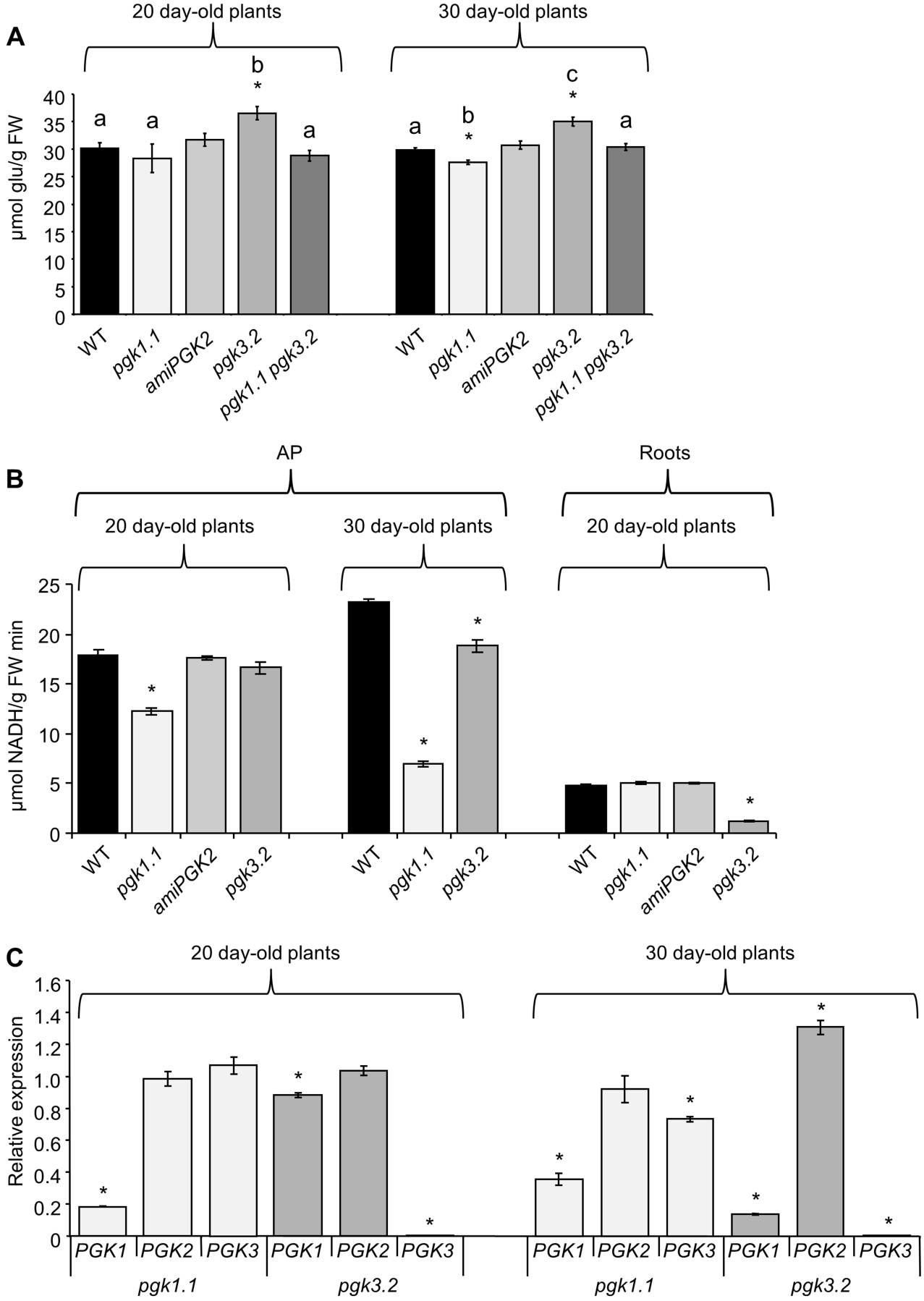


A**B****C**







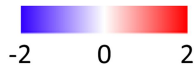


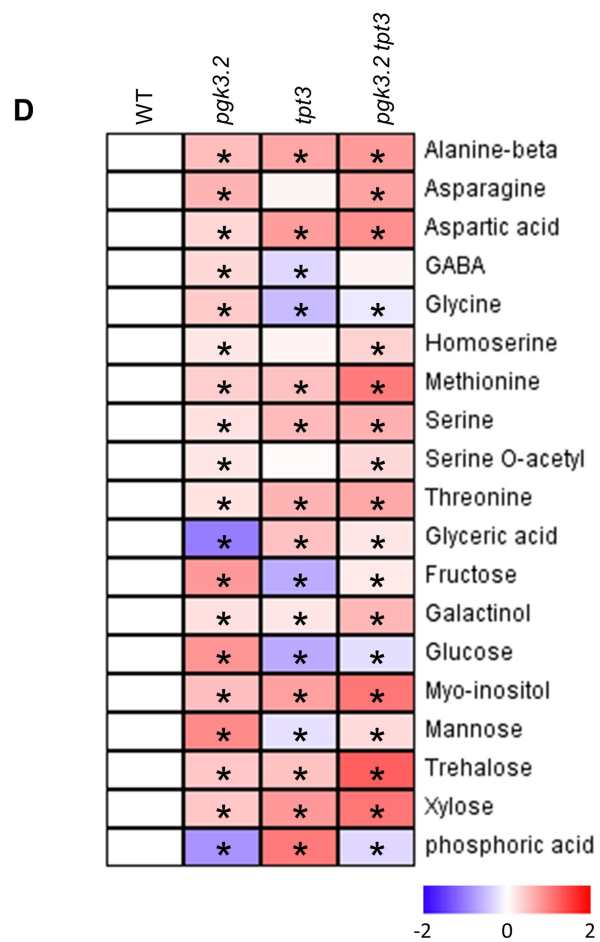
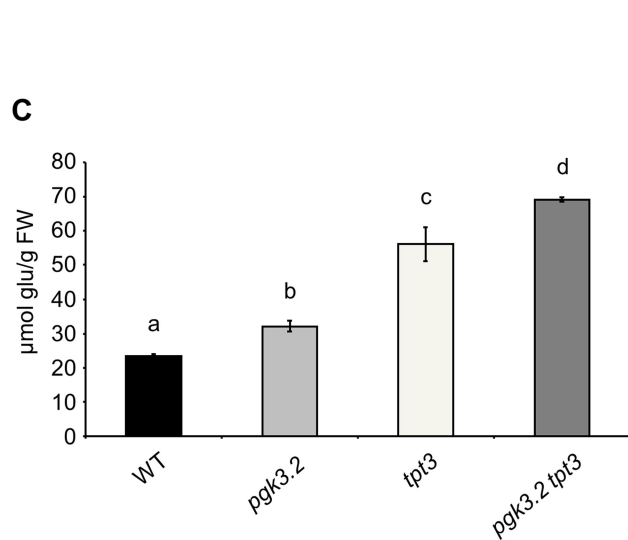
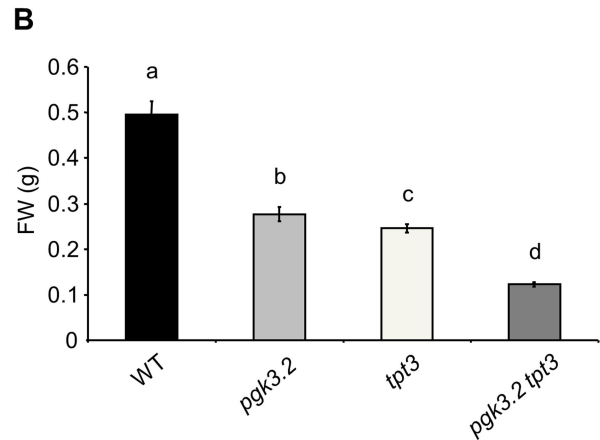
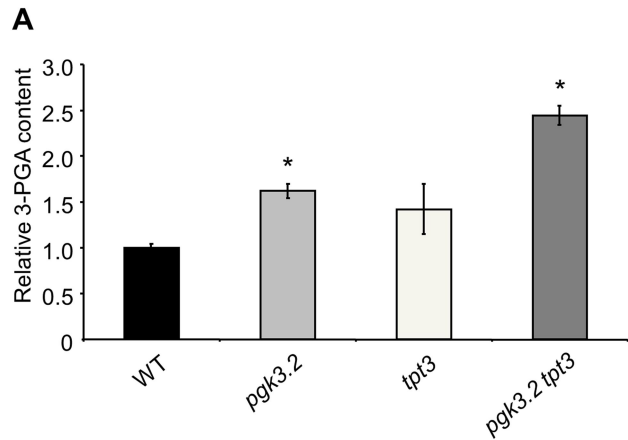
WT	<i>pgk1.1</i>	<i>pgk3.2</i>	<i>pgk1.1 pgk3.2</i>	<i>amiPGK2</i>	
	*			*	Alanine, D, L
	*	*	*	*	Aspartic acid
		*	*		Glutamine
	*				Proline
	*	*			Serine O-Acetyl
	*	*	*	*	Threonine acid
	*	*	*	*	Citric acid
	*	*	*	*	Glyceric acid
	*	*	*		Succinic acid
		*		*	Fructose
	*	*		*	Glucose
			*	*	Raffinose
	*			*	Sucrose
		*		*	Phosphoric acid

AP

WT	<i>pgk1.1</i>	<i>pgk3.2</i>	<i>pgk1.1 pgk3.2</i>	<i>amiPGK2</i>	
	*	*	*	*	Aspartic acid
		*	*		Lysine
	*	*		*	Threonine acid
	*	*	*	*	Citric acid
	*	*		*	Glyceric acid
	*	*	*	*	Succinic acid
	*	*	*	*	Fructose
	*	*	*		Glucose
		*	*	*	Glyceraldehyde-3-P
	*	*	*		Maltitol
	*	*	*	*	Myo-inositol
	*	*	*	*	Raffinose
	*	*	*		Sucrose
	*	*	*	*	Trehalose
		*	*		Phosphoric acid

Roots





Parsed Citations

Ai J, Huang H, Lv X, Tang Z, Chen M, Chen T, Duan W, Sun H, Li Q, Tan R, Liu Y, Duan J, Yang Y, Wei Y, Li Y, Zhou Q (2011) FLNA and PGK1 are two potential markers for progression in hepatocellular carcinoma. Cell Physiol Biochem 27: 207-216

Pubmed: [Author and Title](#)

CrossRef: [Author and Title](#)

Google Scholar: [Author Only](#) [Title Only](#) [Author and Title](#)

Alonso JM, Stepanova AN, Leisse TJ, Kim CJ, Chen H, Shinn P, Stevenson DK, Zimmerman J, Barajas P, Cheuk R, Gadrinab C, Heller C, Jeske A, Koesema E, Meyers CC, Parker H, Prednis L, Ansari Y, Choy N, Deen H, Geralt M, Hazari N, Hom E, Karnes M, Mulholland C, Ndubaku R, Schmidt I, Guzman P, Aguilar-Henonin L, Schmid M, Weigel D, Carter DE, Marchand T, Risseeuw E, Brogden D, Zeko A, Crosby WL, Berry CC, Ecker JR (2003) Genome-wide insertional mutagenesis of Arabidopsis thaliana. Science 301: 653-657

Pubmed: [Author and Title](#)

CrossRef: [Author and Title](#)

Google Scholar: [Author Only](#) [Title Only](#) [Author and Title](#)

Anderson LE, Advani VR (1970) Chloroplast and cytoplasmic enzymes: three distinct isoenzymes associated with the reductive pentose phosphate cycle. Plant Physiol 45: 583-585

Pubmed: [Author and Title](#)

CrossRef: [Author and Title](#)

Google Scholar: [Author Only](#) [Title Only](#) [Author and Title](#)

Anderson LE, Bryant JA, Carol AA (2004) Both chloroplastic and cytosolic phosphoglycerate kinase isozymes are present in the pea leaf nucleus. Protoplasma 223: 103-110

Pubmed: [Author and Title](#)

CrossRef: [Author and Title](#)

Google Scholar: [Author Only](#) [Title Only](#) [Author and Title](#)

Anoman AD, Muñoz-Bertomeu J, Rosa-Téllez S, Flores-Tornero M, Serrano R, Bueso E, Fernie AR, Segura J, Ros R (2015) Plastidial glycolytic glyceraldehyde-3-phosphate dehydrogenase is an important determinant in the carbon and nitrogen metabolism of heterotrophic cells in Arabidopsis. Plant Physiol 169: 1619-1637

Pubmed: [Author and Title](#)

CrossRef: [Author and Title](#)

Google Scholar: [Author Only](#) [Title Only](#) [Author and Title](#)

Archibald JM, Keeling PJ (2003) Comparative genomics. Plant genomes: cyanobacterial genes revealed. Heredity 90: 2-3

Pubmed: [Author and Title](#)

CrossRef: [Author and Title](#)

Google Scholar: [Author Only](#) [Title Only](#) [Author and Title](#)

Blasing OE, Gibon Y, Gunther M, Hohne M, Morcuende R, Osuna D, Thimm O, Usadel B, Scheible WR, Stitt M (2005) Sugars and circadian regulation make major contributions to the global regulation of diurnal gene expression in Arabidopsis. Plant Cell 17: 3257-3281

Pubmed: [Author and Title](#)

CrossRef: [Author and Title](#)

Google Scholar: [Author Only](#) [Title Only](#) [Author and Title](#)

Boer PH, Adra CN, Lau YF, McBurney MW (1987) The testis-specific phosphoglycerate kinase gene pgk-2 is a recruited retroposon. Mol Cell Biol 7: 3107-3112

Pubmed: [Author and Title](#)

CrossRef: [Author and Title](#)

Google Scholar: [Author Only](#) [Title Only](#) [Author and Title](#)

Brice DC, Bryant JA, Dambrauskas G, Drury SC, Littlechild JA (2004) Cloning and expression of cytosolic phosphoglycerate kinase from pea (Pisum sativum L.). J Exp Bot 55: 955-956

Pubmed: [Author and Title](#)

CrossRef: [Author and Title](#)

Google Scholar: [Author Only](#) [Title Only](#) [Author and Title](#)

Brinkmann H, Martin W (1996) Higher-plant chloroplast and cytosolic 3-phosphoglycerate kinases: a case of endosymbiotic gene replacement. Plant Mol Biol 30: 65-75

Pubmed: [Author and Title](#)

CrossRef: [Author and Title](#)

Google Scholar: [Author Only](#) [Title Only](#) [Author and Title](#)

Cascales-Miñana B, Muñoz-Bertomeu J, Flores-Tornero M, Anoman AD, Pertusa J, Alaiz M, Osorio S, Fernie AR, Segura J, Ros R (2013) The phosphorylated pathway of serine biosynthesis is essential both for malegametophyte and embryo development and for root growth in Arabidopsis. Plant Cell 25: 2084-2101

Pubmed: [Author and Title](#)

CrossRef: [Author and Title](#)

Google Scholar: [Author Only](#) [Title Only](#) [Author and Title](#)

Clough SJ, Bent AF (1998) Floral dip: a simplified method for Agrobacterium-mediated transformation of Arabidopsis thaliana. Plant J 16: 735-743

Pubmed: [Author and Title](#)
CrossRef: [Author and Title](#)
Google Scholar: [Author Only Title Only Author and Title](#)

Curtis MD, Grossniklaus U (2003) A gateway cloning vector set for high-throughput functional analysis of genes in planta. Plant Physiol 133: 462-469

Pubmed: [Author and Title](#)
CrossRef: [Author and Title](#)
Google Scholar: [Author Only Title Only Author and Title](#)

Chen M, Thelen JJ (2010) The plastid isoform of triose phosphate isomerase is required for the postgerminative transition from heterotrophic to autotrophic growth in Arabidopsis. Plant Cell 22: 77-90

Pubmed: [Author and Title](#)
CrossRef: [Author and Title](#)
Google Scholar: [Author Only Title Only Author and Title](#)

Cheng SF, Huang YP, Chen LH, Hsu YH, Tsai CH (2013) Chloroplast phosphoglycerate kinase is involved in the targeting of Bamboo mosaic virus to chloroplasts in Nicotiana benthamiana plants. Plant Physiol 163: 1598-1608

Pubmed: [Author and Title](#)
CrossRef: [Author and Title](#)
Google Scholar: [Author Only Title Only Author and Title](#)

Chiarelli LR, Morera SM, Bianchi P, Fermo E, Zanella A, Galizzi A, Valentini G (2012) Molecular insights on pathogenic effects of mutations causing phosphoglycerate kinase deficiency. PLoS One 7: e32065

Pubmed: [Author and Title](#)
CrossRef: [Author and Title](#)
Google Scholar: [Author Only Title Only Author and Title](#)

Czechowski T, Stitt M, Altmann T, Udvardi MK, Scheible WR (2005) Genome-wide identification and testing of superior reference genes for transcript normalization in Arabidopsis. Plant Physiol 139: 5-17

Pubmed: [Author and Title](#)
CrossRef: [Author and Title](#)
Google Scholar: [Author Only Title Only Author and Title](#)

Danshina PV, Geyer CB, Dai Q, Goulding EH, Willis WD, Kitto GB, McCarrey JR, Eddy EM, O'Brien DA (2010) Phosphoglycerate kinase 2 (PGK2) is essential for sperm function and male fertility in mice. Biol Reprod 82: 136-145

Pubmed: [Author and Title](#)
CrossRef: [Author and Title](#)
Google Scholar: [Author Only Title Only Author and Title](#)

Emanuelsson O, Nielsen H, von Heijne G (1999) ChloroP, a neural network-based method for predicting chloroplast transit peptides and their cleavage sites. Protein Sci 8: 978-984

Pubmed: [Author and Title](#)
CrossRef: [Author and Title](#)
Google Scholar: [Author Only Title Only Author and Title](#)

Faus I, Zabalza A, Santiago J, Nebauer SG, Royuela M, Serrano R, Gadea J (2015) Protein kinase GCN2 mediates responses to glyphosate in Arabidopsis. BMC Plant Biol 15: 14

Pubmed: [Author and Title](#)
CrossRef: [Author and Title](#)
Google Scholar: [Author Only Title Only Author and Title](#)

Fermani S, Sparla F, Falini G, Martelli PL, Casadio R, Pupillo P, Ripamonti A, Trost P (2007) Molecular mechanism of thioredoxin regulation in photosynthetic A2B2-glyceraldehyde-3-phosphate dehydrogenase. Proc Natl Acad Sci USA 104: 11109-11114

Pubmed: [Author and Title](#)
CrossRef: [Author and Title](#)
Google Scholar: [Author Only Title Only Author and Title](#)

Fischer K, Weber A (2002) Transport of carbon in non-green plastids. Trends Plant Sci 7: 345-351

Pubmed: [Author and Title](#)
CrossRef: [Author and Title](#)
Google Scholar: [Author Only Title Only Author and Title](#)

Flores-Tornero M, Anoman AD, Rosa-Télliz S, Toujani W, Weber AP, Eisenhut M, Kurz S, Alseekh S, Fernie AR, Muñoz-Bertomeu J, Ros R (2017) Overexpression of the triose phosphate translocator (TPT) complements the abnormal metabolism and development of plastidial glycolytic glyceraldehyde-3-phosphate dehydrogenase mutants. Plant J 89: 1146-1158

Pubmed: [Author and Title](#)
CrossRef: [Author and Title](#)
Google Scholar: [Author Only Title Only Author and Title](#)

Guo L, Devaiah SP, Narasimhan R, Pan X, Zhang Y, Zhang W, Wang X (2012) Cytosolic glyceraldehyde-3-phosphate dehydrogenases interact with phospholipase D5 to transduce hydrogen peroxide signals in the Arabidopsis response to stress. Plant Cell 24: 2200-2212

Pubmed: [Author and Title](#)
CrossRef: [Author and Title](#)
Google Scholar: [Author Only Title Only Author and Title](#)

Guo L, Ma F, Wei F, Fanella B, Allen DK, Wang X (2014) Cytosolic phosphorylating glyceraldehyde-3-phosphate dehydrogenases affect Arabidopsis cellular metabolism and promote seed oil accumulation. Plant Cell 26: 3023-3035

Pubmed: [Author and Title](#)

CrossRef: [Author and Title](#)

Google Scholar: [Author Only](#) [Title Only](#) [Author and Title](#)

Hajirezaei MR, Biemelt S, Peisker M, Lytovchenko A, Fernie AR, Sonnewald U (2006) The influence of cytosolic phosphorylating glyceraldehyde 3-phosphate dehydrogenase (GAPC) on potato tuber metabolism. J Exp Bot 57: 2363-2377

Pubmed: [Author and Title](#)

CrossRef: [Author and Title](#)

Google Scholar: [Author Only](#) [Title Only](#) [Author and Title](#)

Han S, Wang Y, Zheng X, Jia Q, Zhao J, Bai F, Hong Y, Liu Y (2015) Cytoplasmic glyceraldehyde-3-phosphate dehydrogenases interact with ATG3 to negatively regulate autophagy and immunity in Nicotiana benthamiana. Plant Cell 27: 1316-1331

Pubmed: [Author and Title](#)

CrossRef: [Author and Title](#)

Google Scholar: [Author Only](#) [Title Only](#) [Author and Title](#)

Holtgreffe S, Gohlke J, Starmann J, Druce S, Klocke S, Altmann B, Wojtera J, Lindermayr C, Scheibe R (2008) Regulation of plant cytosolic glyceraldehyde 3-phosphate dehydrogenase isoforms by thiol modifications. Physiol Plant 133: 211-228

Pubmed: [Author and Title](#)

CrossRef: [Author and Title](#)

Google Scholar: [Author Only](#) [Title Only](#) [Author and Title](#)

Hwang TL, Liang Y, Chien KY, Yu JS (2006) Overexpression and elevated serum levels of phosphoglycerate kinase 1 in pancreatic ductal adenocarcinoma. Proteomics 6: 2259-2272

Pubmed: [Author and Title](#)

CrossRef: [Author and Title](#)

Google Scholar: [Author Only](#) [Title Only](#) [Author and Title](#)

Joshi R, Karan R, Singla-Pareek SL, Pareek A (2016) Ectopic expression of Pokkali phosphoglycerate kinase-2 (OsPGK2-P) improves yield in tobacco plants under salinity stress. Plant Cell Rep 35: 27-41

Pubmed: [Author and Title](#)

CrossRef: [Author and Title](#)

Google Scholar: [Author Only](#) [Title Only](#) [Author and Title](#)

Kopka J, Schauer N, Krueger S, Birkemeyer C, Usadel B, Bergmüller E, Dormann P, Weckwerth W, Gibon Y, Stitt M, Willmitzer L, Fernie AR, Steinhauser D (2005) GMD@CSB.DB: the Golm Metabolome Database. Bioinformatics 21: 1635-1638

Pubmed: [Author and Title](#)

CrossRef: [Author and Title](#)

Google Scholar: [Author Only](#) [Title Only](#) [Author and Title](#)

Köpke-Secundo E, Molnar I, Schnarrenberger C (1990) Isolation and characterization of the cytosolic and chloroplastic 3-phosphoglycerate kinase from spinach leaves. Plant Physiol 93: 40-47

Pubmed: [Author and Title](#)

CrossRef: [Author and Title](#)

Google Scholar: [Author Only](#) [Title Only](#) [Author and Title](#)

Krietsch WK, Bucher T (1970) 3-phosphoglycerate kinase from rabbit skeletal muscle and yeast. Eur J Biochem 17: 568-580

Pubmed: [Author and Title](#)

CrossRef: [Author and Title](#)

Google Scholar: [Author Only](#) [Title Only](#) [Author and Title](#)

Lay AJ, Jiang XM, Kisker O, Flynn E, Underwood A, Condron R, Hogg PJ (2000) Phosphoglycerate kinase acts in tumour angiogenesis as a disulphide reductase. Nature 408: 869-873

Pubmed: [Author and Title](#)

CrossRef: [Author and Title](#)

Google Scholar: [Author Only](#) [Title Only](#) [Author and Title](#)

Lin JW, Ding MP, Hsu YH, Tsai CH (2007) Chloroplast phosphoglycerate kinase, a gluconeogenic enzyme, is required for efficient accumulation of Bamboo mosaic virus. Nucleic Acids Res 35: 424-432

Pubmed: [Author and Title](#)

CrossRef: [Author and Title](#)

Google Scholar: [Author Only](#) [Title Only](#) [Author and Title](#)

Lisec J, Schauer N, Kopka J, Willmitzer L, Fernie AR (2006) Gas chromatography mass spectrometry-based metabolite profiling in plants. Nat Protoc 1: 387-396

Pubmed: [Author and Title](#)

CrossRef: [Author and Title](#)

Google Scholar: [Author Only](#) [Title Only](#) [Author and Title](#)

Liu D, Li W, Cheng J, Hou L (2015) AtPGK2, a member of PGKs gene family in Arabidopsis, has a positive role in salt stress tolerance. Plant Cell Tissue Organ Culture 120: 251-262

Pubmed: [Author and Title](#)

CrossRef: [Author and Title](#)

Google Scholar: [Author Only](#) [Title Only](#) [Author and Title](#)

Lobler M (1998) Two phosphoglycerate kinase cDNAs from *Arabidopsis thaliana*. DNA Sequence 8: 247-252

Pubmed: [Author and Title](#)

CrossRef: [Author and Title](#)

Google Scholar: [Author Only](#) [Title Only](#) [Author and Title](#)

Longstaff M, Raines CA, McMorrow EM, Bradbeer JW, Dyer TA (1989) Wheat phosphoglycerate kinase: evidence for recombination between the genes for the chloroplastic and cytosolic enzymes. Nucleic Acids Res 17: 6569-6580

Pubmed: [Author and Title](#)

CrossRef: [Author and Title](#)

Google Scholar: [Author Only](#) [Title Only](#) [Author and Title](#)

Luedemann A, Strassburg K, Erban A, Kopka J (2008) TagFinder for the quantitative analysis of gas chromatography-mass spectrometry (GC-MS)-based metabolite profiling experiments. Bioinformatics 24: 732-737

Pubmed: [Author and Title](#)

CrossRef: [Author and Title](#)

Google Scholar: [Author Only](#) [Title Only](#) [Author and Title](#)

McCarrey JR, Thomas K (1987) Human testis-specific PGK gene lacks introns and possesses characteristics of a processed gene. Nature 326: 501-505

Pubmed: [Author and Title](#)

CrossRef: [Author and Title](#)

Google Scholar: [Author Only](#) [Title Only](#) [Author and Title](#)

McCormick AJ, Kruger NJ (2015) Lack of fructose 2,6-bisphosphate compromises photosynthesis and growth in *Arabidopsis* in fluctuating environments. Plant J 81: 670-683

Pubmed: [Author and Title](#)

CrossRef: [Author and Title](#)

Google Scholar: [Author Only](#) [Title Only](#) [Author and Title](#)

McMorrow EM, Bradbeer JW (1990) Separation, purification, and comparative properties of chloroplast and cytoplasmic phosphoglycerate kinase from barley leaves. Plant Physiol 93: 374-383

Pubmed: [Author and Title](#)

CrossRef: [Author and Title](#)

Google Scholar: [Author Only](#) [Title Only](#) [Author and Title](#)

McWilliam H, Li W, Uludag M, Squizzato S, Park YM, Buso N, Cowley AP, Lopez R (2013) Analysis Tool Web Services from the EMBL-EBI. Nucleic Acids Res 41: W597-W600

Pubmed: [Author and Title](#)

CrossRef: [Author and Title](#)

Google Scholar: [Author Only](#) [Title Only](#) [Author and Title](#)

Morisse S, Michelet L, Bedhomme M, Marchand CH, Calvaresi M, Trost P, Fermani S, Zaffagnini M, Lemaire SD (2014) Thioredoxin-dependent redox regulation of chloroplastic phosphoglycerate kinase from *Chlamydomonas reinhardtii*. J Biol Chem 289: 30012-30024

Pubmed: [Author and Title](#)

CrossRef: [Author and Title](#)

Google Scholar: [Author Only](#) [Title Only](#) [Author and Title](#)

Muñoz-Bertomeu J, Cascales-Miñana B, Irlés-Segura A, Mateu I, Nunes-Nesi A, Fernie AR, Segura J, Ros R (2010) The plastidial glyceraldehyde-3-phosphate dehydrogenase is critical for viable pollen development in *Arabidopsis*. Plant Physiol 152: 1830-1841

Pubmed: [Author and Title](#)

CrossRef: [Author and Title](#)

Google Scholar: [Author Only](#) [Title Only](#) [Author and Title](#)

Muñoz-Bertomeu J, Cascales-Miñana B, Mulet JM, Baroja-Fernandez E, Pozueta-Romero J, Kuhn JM, Segura J, Ros R (2009) Plastidial glyceraldehyde-3-phosphate dehydrogenase deficiency leads to altered root development and affects the sugar and amino acid balance in *Arabidopsis*. Plant Physiol 151: 541-558

Pubmed: [Author and Title](#)

CrossRef: [Author and Title](#)

Google Scholar: [Author Only](#) [Title Only](#) [Author and Title](#)

Myouga F, Akiyama K, Motohashi R, Kuromori T, Ito T, Iizumi H, Ryusui R, Sakurai T, Shinozaki K (2010) The Chloroplast Function Database: a large-scale collection of *Arabidopsis* Ds/Spm- or T-DNA-tagged homozygous lines for nuclear-encoded chloroplast proteins, and their systematic phenotype analysis. Plant J 61: 529-542

Pubmed: [Author and Title](#)

CrossRef: [Author and Title](#)

Google Scholar: [Author Only](#) [Title Only](#) [Author and Title](#)

Ouibrahim L, Mazier M, Estevan J, Pagny G, Decroocq V, Desbiez C, Moretti A, Gallois JL, Caranta C (2014) Cloning of the *Arabidopsis* *rwm1* gene for resistance to Watermelon mosaic virus points to a new function for natural virus resistance genes. Plant J 79: 705-716

Pubmed: [Author and Title](#)

CrossRef: [Author and Title](#)

Google Scholar: [Author Only](#) [Title Only](#) [Author and Title](#)

- Paul MJ, Pellny TK (2003) Carbon metabolite feedback regulation of leaf photosynthesis and development. J Exp Bot 54: 539-547**
Pubmed: [Author and Title](#)
CrossRef: [Author and Title](#)
Google Scholar: [Author Only Title Only Author and Title](#)
- Petersen J, Brinkmann H, Cerff R (2003) Origin, evolution, and metabolic role of a novel glycolytic GAPDH enzyme recruited by land plant plastids. J Mol Evol 57: 16-26**
Pubmed: [Author and Title](#)
CrossRef: [Author and Title](#)
Google Scholar: [Author Only Title Only Author and Title](#)
- Plaxton WC (1996) The organization and regulation of plant glycolysis. Annu Rev Plant Physiol Plant Mol Biol 47: 185-214**
Pubmed: [Author and Title](#)
CrossRef: [Author and Title](#)
Google Scholar: [Author Only Title Only Author and Title](#)
- Popanda O, Fox G, Thielmann HW (1998) Modulation of DNA polymerases α , δ and ϵ by lactate dehydrogenase and 3-phosphoglycerate kinase. Biochim Biophys Acta 1397: 102-117**
Pubmed: [Author and Title](#)
CrossRef: [Author and Title](#)
Google Scholar: [Author Only Title Only Author and Title](#)
- Prabhakar V, Lottgert T, Geimer S, Dormann P, Kruger S, Vijayakumar V, Schreiber L, Gobel C, Feussner K, Feussner I, Marin K, Staehr P, Bell K, Flugge UI, Hausler RE (2010) Phosphoenolpyruvate provision to plastids is essential for gametophyte and sporophyte development in Arabidopsis thaliana. Plant Cell 22: 2594-2617**
Pubmed: [Author and Title](#)
CrossRef: [Author and Title](#)
Google Scholar: [Author Only Title Only Author and Title](#)
- Rius SP, Casati P, Iglesias AA, Gomez-Casati DF (2006) Characterization of an Arabidopsis thaliana mutant lacking a cytosolic non-phosphorylating glyceraldehyde-3-phosphate dehydrogenase. Plant Mol Biol 61: 945-957**
Pubmed: [Author and Title](#)
CrossRef: [Author and Title](#)
Google Scholar: [Author Only Title Only Author and Title](#)
- Saitou N, Nei M (1987) The neighbor-joining method: a new method for reconstructing phylogenetic trees. Mol Biol Evol 4: 406-425**
Pubmed: [Author and Title](#)
CrossRef: [Author and Title](#)
Google Scholar: [Author Only Title Only Author and Title](#)
- Sambrook J, Russell DW (2001) Molecular cloning: A laboratory manual, Ed 3. Cold Spring Harbor Laboratory Press, Cold Spring Harbor, NY**
Pubmed: [Author and Title](#)
CrossRef: [Author and Title](#)
Google Scholar: [Author Only Title Only Author and Title](#)
- Scholl RL, May ST, Ware DH (2000) Seed and molecular resources for Arabidopsis. Plant Physiol 124: 1477-1480**
Pubmed: [Author and Title](#)
CrossRef: [Author and Title](#)
Google Scholar: [Author Only Title Only Author and Title](#)
- Shih MC, Lazar G, Goodman HM (1986) Evidence in favor of the symbiotic origin of chloroplasts: primary structure and evolution of tobacco glyceraldehyde-3-phosphate dehydrogenases. Cell 47: 73-80**
Pubmed: [Author and Title](#)
CrossRef: [Author and Title](#)
Google Scholar: [Author Only Title Only Author and Title](#)
- Smith AM, Stitt M (2007) Coordination of carbon supply and plant growth. Plant Cell Environ 30: 1126-1149**
Pubmed: [Author and Title](#)
CrossRef: [Author and Title](#)
Google Scholar: [Author Only Title Only Author and Title](#)
- Sparla F, Zaffagnini M, Wedel N, Scheibe R, Pupillo P, Trost P (2005) Regulation of photosynthetic GAPDH dissected by mutants. Plant Physiol 138: 2210-2219**
Pubmed: [Author and Title](#)
CrossRef: [Author and Title](#)
Google Scholar: [Author Only Title Only Author and Title](#)
- Staehr P, Lottgert T, Christmann A, Krueger S, Rosar C, Rolcik J, Novak O, Strnad M, Bell K, Weber AP, Flugge UI, Hausler RE (2014) Reticulate leaves and stunted roots are independent phenotypes pointing at opposite roles of the phosphoenolpyruvate/phosphate translocator defective in cue1 in the plastids of both organs. Front Plant Sci 5: 1-5**
Pubmed: [Author and Title](#)
CrossRef: [Author and Title](#)
Google Scholar: [Author Only Title Only Author and Title](#)
- Stitt M, Lunn J, Usadel B (2010) Arabidopsis and primary photosynthetic metabolism: more than the icing on the cake. Plant J 61: 1067-1091**

Pubmed: [Author and Title](#)
CrossRef: [Author and Title](#)
Google Scholar: [Author Only Title Only Author and Title](#)

Tamura K, Stecher G, Peterson D, Filipski A, Kumar S (2013) MEGA6: Molecular Evolutionary Genetics Analysis version 6.0. Mol Biol Evol 30: 2725-2729

Pubmed: [Author and Title](#)
CrossRef: [Author and Title](#)
Google Scholar: [Author Only Title Only Author and Title](#)

Troncoso-Ponce MA, Garces R, Martinez-Force E (2010) Glycolytic enzymatic activities in developing seeds involved in the differences between standard and low oil content sunflowers (*Helianthus annuus* L.). Plant Physiol Biochem 48: 961-965

Pubmed: [Author and Title](#)
CrossRef: [Author and Title](#)
Google Scholar: [Author Only Title Only Author and Title](#)

Troncoso-Ponce MA, Kruger NJ, Ratcliffe G, Garces R, Martinez-Force E (2009) Characterization of glycolytic initial metabolites and enzyme activities in developing sunflower (*Helianthus annuus* L.) seeds. Phytochemistry 70: 1117-1122

Pubmed: [Author and Title](#)
CrossRef: [Author and Title](#)
Google Scholar: [Author Only Title Only Author and Title](#)

Troncoso-Ponce MA, Rivoal J, Venegas-Caleron M, Dorion S, Sanchez R, Cejudo FJ, Garces R, Martinez-Force E (2012) Molecular cloning and biochemical characterization of three phosphoglycerate kinase isoforms from developing sunflower (*Helianthus annuus* L.) seeds. Phytochemistry 79: 27-38

Pubmed: [Author and Title](#)
CrossRef: [Author and Title](#)
Google Scholar: [Author Only Title Only Author and Title](#)

Wakao S, Chin BL, Ledford HK, Dent RM, Casero D, Pellegrini M, Merchant SS, Niyogi KK (2014) Phosphoprotein SAK1 is a regulator of acclimation to singlet oxygen in *Chlamydomonas reinhardtii*. Elife 3: e02286

Pubmed: [Author and Title](#)
CrossRef: [Author and Title](#)
Google Scholar: [Author Only Title Only Author and Title](#)

Willard HF, Goss SJ, Holmes MT, Munroe DL (1985) Regional localization of the phosphoglycerate kinase gene and pseudogene on the human X chromosome and assignment of a related DNA sequence to chromosome 19. Hum Genet 71: 138-143

Pubmed: [Author and Title](#)
CrossRef: [Author and Title](#)
Google Scholar: [Author Only Title Only Author and Title](#)

Zhao Z, Assmann SM (2011) The glycolytic enzyme, phosphoglycerate mutase, has critical roles in stomatal movement, vegetative growth, and pollen production in *Arabidopsis thaliana*. J Exp Bot 62: 5179-5189

Pubmed: [Author and Title](#)
CrossRef: [Author and Title](#)
Google Scholar: [Author Only Title Only Author and Title](#)

Zieker D, Konigsrainer I, Traub F, Nieselt K, Knapp B, Schillinger C, Stirnkorb C, Fend F, Northoff H, Kupka S, Brucher BL, Konigsrainer A (2008) PGK1 a potential marker for peritoneal dissemination in gastric cancer. Cell Physiol Biochem 21: 429-436

Pubmed: [Author and Title](#)
CrossRef: [Author and Title](#)
Google Scholar: [Author Only Title Only Author and Title](#)

Zieker D, Konigsrainer I, Weinreich J, Beckert S, Glatzle J, Nieselt K, Buhler S, Loffler M, Gaedcke J, Northoff H, Mannheim JG, Wiehr S, Pichler BJ, von Weyhern C, Brucher BL, Konigsrainer A (2010) Phosphoglycerate kinase 1 promoting tumor progression and metastasis in gastric cancer - detected in a tumor mouse model using positron emission tomography/magnetic resonance imaging. Cell Physiol Biochem 26: 147-154

Pubmed: [Author and Title](#)
CrossRef: [Author and Title](#)
Google Scholar: [Author Only Title Only Author and Title](#)